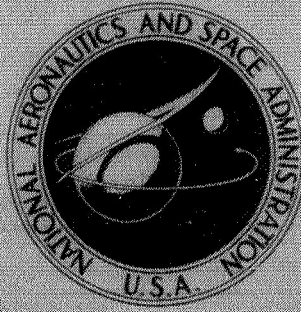


N71-11226

NASA CONTRACTOR  
REPORT



NASA CR-1667

NASA CR-1667

CASE FILE  
COPY



SPECTROSCOPIC STUDIES  
OF INTERSTELLAR GRAINS

*by Fred M. Johnson*

Prepared by  
ELECTRO-OPTICAL SYSTEMS  
Pasadena, Calif. 91107  
for

NATIONAL AERONAUTICS AND SPACE ADMINISTRATION • WASHINGTON, D. C. • NOVEMBER 1970

1. Report No. NASA CR-1667	2. Government Accession No.	3. Recipient's Catalog No.	
4. Title and Subtitle SPECTROSCOPIC STUDIES OF INTERSTELLAR GRAINS		5. Report Date November 1970	
		6. Performing Organization Code	
7. Author(s) Fred M. Johnson		8. Performing Organization Report No. EOS 4022	
9. Performing Organization Name and Address Electro-Optical Systems Pasadena, California 91107		10. Work Unit No.	
		11. Contract or Grant No. NASW-1803	
12. Sponsoring Agency Name and Address National Aeronautics and Space Administration Washington, D. C. 20546		13. Type of Report and Period Covered Contractor Report	
		14. Sponsoring Agency Code	
15. Supplementary Notes			
16. Abstract Results of an extensive experimental spectroscopic survey are presented directed towards laboratory simulation of 25 diffuse interstellar bands. Hundreds of compounds in a multitude of solvents were extensively studied. The Shpol'skii matrix isolation technique was successfully used on a number of Tetrabenzporphins, of which the molecule Bispyridylmagnesiumtetrabenzoporphine (X) gave a fit to $\pm 2\text{\AA}$ for 16 diffuse lines. In addition, good correlation with line width and intensity was obtained for all lines. Additional corroborative evidence was obtained from IR absorption measurements on molecule X. An energy level diagram was constructed based on two excited electronic states where all 25 diffuse lines correspond to vibronic transitions, using the strongest measured IR lines. Implications of those results and the physical conditions under which these molecules are formed are discussed. Tabulations are given of experimental spectroscopic absorption and fluorescence data for a large variety of porphyrins studied under this program.			
17. Key Words (Selected by Author(s)) Laboratory Spectroscopic Simulation - Interstellar lines - Porphyrins - Bispyridylmagnesiumtetrabenzoporphine (X) - Reddending		18. Distribution Statement  Unclassified - Unlimited	
19. Security Classif. (of this report)  Unclassified	20. Security Classif. (of this page)  Unclassified	21. No. of Pages  109	22. Price*  \$3.00



## TABLE OF CONTENTS

<u>Section</u>	<u>Page</u>
1. INTRODUCTION	1
1.1 Introduction	1
1.2 Summary of Results	1
1.3 Background	3
1.4 Experimental Approach Leading Towards the Identification of Molecule $\chi$	5
1.4.1 The Experimental Plan	5
1.5 Acknowledgements	7
2. EXPERIMENTAL RESULTS	8
2.1 Description of Equipment and Techniques	8
2.2 Summary of Low Temperature Matrix Isolation Data (Technique A)	9
2.4 Detailed Discussion of Results Using Technique A	24
2.4.1 Chemical Structure	24
2.4.2 Temperature Effects	26
2.4.3 Matrix Effect (Technique A)	26
2.4.4 Mixture Effect	29
2.5 Detailed Results Using Technique A (Porphyrins, Set A) and Discussion	36
3. RESULTS--CONTINUED	48
3.1 The Tetrabenzporphines, Technique B	48
3.2 IR Spectra	58
3.3 Thermodynamic Tests on Molecule $\chi$	64



## TABLE OF CONTENTS

<u>Section</u>	<u>Page</u>
3.4 Fluorescence Data	66
3.5 Complexing of Porphyrin Molecules	66
3.6 Reddening	70
3.7 Discussion on the Origin of $\chi$	77
3.8 Interstellar Microwave Emission from $H_2O$	79
3.9 Analysis of Data	80
3.10 Line Width	85
3.11 Summary of Energy Level Diagram	89
3.12 Interstellar Abundances of Molecule $\chi$	90
4. CONCLUSION AND SUMMARY	91
4.1 Conclusion and Summary	91
APPENDIX I	93
SCIENTIFIC REPORT NO. 1	95

## LIST OF ILLUSTRATIONS

<u>Figure No.</u>		<u>Page</u>
1	The Interstellar Molecule X ( $\text{MgC}_{46}\text{H}_{30}\text{N}_6$ ).	2
2	Schematic Diagram of Experimental Arrangement.	10
3	Photograph of Experimental Equipment Showing Overall Layout. Beckman Spectrophotometer and Automatic Mortar Grinding Equipment may be Seen in the Background.	11
4	Photograph of Experimental Equipment. Following details are shown: Sensitive photodetection equipment showing light source, dewar, scanning spectrophotometer, lock-in detector, and strip-chart recorder.	12
5	Solution Data Compared with Powder Matrixes at 77°K	16
6	Porphyrin Powder Suspensions (Technique A).	18
7	Powder vs Liquid Suspension.	19
8	Microscope Photograph Enlargement of Specimen Containing Admixture of Porphin + Perylene + Murray.	20
9	Microscope Photograph Enlargement of Specimen Containing Admixture of Perylene + Murray.	21
10	Microscope Photograph Enlargement of Specimen Containing Admixture of Sample No. 2 with Meteorite Powder from Orgueil.	22
11	Absorption Spectra of Ovalene at 77°K (Technique A).	28
12	Typical Absorption Spectra (Technique A).	33
13	Temperature Effects on Absorption Spectra.	34

# LIST OF ILLUSTRATIONS

(Continued)

<u>Figure No.</u>		<u>Page</u>
14	52 Aromatic Hydrocarbon Composite Spectrum-- in Powder Matrix Suspension (Technique A).	35
15.	Molecule $\chi$ : Typical Room Temperature Data-- See Text.	49
16	A - MgTBP in EPA (3mm cell) B - MgTBP + 2CN in EPA liquid glass at 77°K C - MgTBP in EPA Room Temperature (1 cm cell).	50
17	Laboratory Measurement Soret Band of Molecule $\chi$ .	56
18	Molecular Beam Apparatus Equipment to Demonstrate Sublimation of $\chi$ Molecules at ~500°C.	65
19	Molecular "add-ons" to MgTBP.	71
20	Aggregation of $\chi$ molecules to simulate reddening A - No aggregation B - Various degrees of $\chi$ association C - " " " " " Note break in slope on short wavelength side of 4430 in Curve C.	74
21	Energy level diagram: Experimental and Astro- nomical data.	81
22	"Boltzmann" plot for $\chi'$ (presumably an aggregate of $\chi$ ).	83
23	"Boltzmann" plot for $\chi$ .	84

# LIST OF TABLES

<u>Table No.</u>		<u>Page</u>
I	PORPHIN ABSORPTION MAXIMA	14
II	PERYLENE ABSORPTION MAXIMA	15
III	PORPHYRIN COMPOUNDS STUDIED	23
IV	EXAMINED HYDROCARBONS	30
V	EXPERIMENTAL RESULTS--LIQUID NITROGEN SPECTRA OF PORPHYRINS (TECHNIQUE A)	38
VI	TBP & Pc SURVEY DATA	51
VII	LABORATORY MEASUREMENTS ON MOLECULE $\chi$ AT 77°K	57
VIII	IR ABSORPTION MEASUREMENTS	60
IX	IR ASTRONOMICAL ABSORPTION SPECTRA	61
X	INTERSTELLAR IR LINES AND LABORATORY SPECTRA	62
XI	INTERPRETATION OF IR SPECTRA	63
XII	FLUORESCENCE DATA	67



## SECTION 1

### INTRODUCTION

#### 1.1 INTRODUCTION

This report comprises the second phase of a research project directed toward an experimental and theoretical study pertaining to the chemical identification of the interstellar "dust". The first phase of the effort was reported on in a previous final report dated August 31, 1967 under NASA Contract NASW1450. It was then shown that a possible solution to the chemical identification could be found by means of a class of compounds called porphyrins. Moreover, whereas in the first phase the emphasis was on literature search, analysis, and preliminary experiments, the second phase concentrated primarily on the experimental aspects of the program.

#### 1.2 SUMMARY OF RESULTS

The key result of this program was the definitive chemical identification of the dominant component of the interstellar medium responsible for the diffuse interstellar lines and reddening. This compound is the ultra-stable porphyrin molecule:

##### BISPYRIDYLMAGNESIUMTETRABENZOPORPHINE

$\text{MgC}_{46}\text{H}_{30}\text{N}_6$  (abbreviated to  $\chi$ ). Figure 1 shows its structure. This identification rests on 16 laboratory coincidences of the interstellar diffuse lines with low temperature laboratory data on  $\chi$ , plus 6 coincidences of IR astronomical lines and laboratory room temperature spectra, making a total of 22 lines. In addition, good correlation of line width and intensity ratios of the lines was obtained. Interstellar reddening was simulated in laboratory by clustering  $\chi$  molecules. All additional

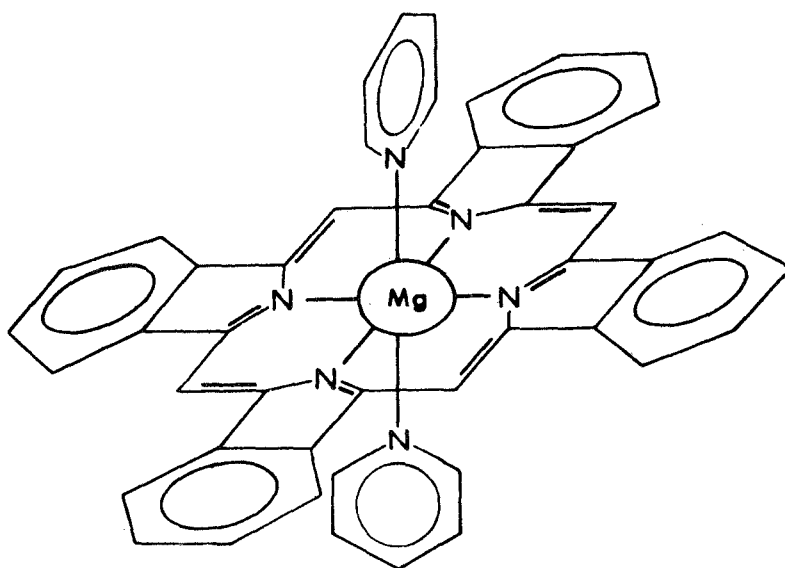


Figure 1. The Interstellar Molecule  $\chi$  ( $\text{MgC}_{46}\text{H}_{30}\text{N}_6$ )

interstellar lines not observed in our laboratory spectra are explicable in terms of vibronic transitions. A self-consistent energy level diagram showing the major vibronic and electronic transitions can now be constructed. It can readily be shown that the a priori random probability of spectral assignments of the X molecular spectra plus line width and intensity correlation with the spectra of the diffuse interstellar lines is conservatively  $10^{50}:1$ . A theoretical discussion of the experimentally produced interstellar "reddening" phenomena is given in this report. For a summary of the results and their implications see Scientific Report No. 1 (in the Appendix). (The extensive results using Technique A could be passed over on the first reading.)

### 1.3 BACKGROUND

It is therefore felt that the major task of identifying the molecule has been accomplished. With this solution however, a host of other problems have been opened up, like a Pandora's box, which require answers. Indeed the laboratory spectrum can still be improved by an order of magnitude leading toward determinations of interstellar environment and "molecular add-ons" to the primary interstellar molecule chi (X).

One scientific paper was presented at the 129th Astronomical Society Meeting giving our preliminary results in April 1969. Additional papers are being prepared, one of which, included with this report has been submitted for publication.

Since for the last 30 years a large number of theories pertaining to the chemical nature of the dust have been proposed, it might be appropriate to very briefly review the situation. Reference is made to a paper by the author entitled "Interstellar Matter", which appeared as Scientific Report No. 1 in the final report of August 1967 and which has meantime

appeared in print.\* Briefly the problem is this: one not only has to match 25 diffuse interstellar lines as far as wavelengths are concerned, but also as far as intensity. In addition, the fact that interstellar line widths vary from  $40\text{\AA}$  to  $1\text{\AA}$  argues against identification of small molecules whose lines are sharp. Predissociation bands of triatomic molecules, as proposed by G. Herzberg, have so far not succeeded. Another competing theory might be atoms suspended in matrixes; proponents of this model were H. P. Broida and G. W. Robinson. The difficulty with this model is that not only have no coincidences been observed, but the major problem is the variation of wavelength maxima for different matrixes (by as much as  $100\text{\AA}$ ). Since the interstellar medium yields a set of lines whose positions are invariant to  $0.1\text{\AA}$ , it is impossible to imagine a unique matrix that would satisfy the condition. Other theories can more readily be eliminated on very elementary considerations. This leaves the remaining possibility, viz., that large molecules or a cluster of these large molecules make up the interstellar dust, and this is indeed what we have tried to show in this final report. Namely, that the interstellar medium contains among other gas components, hydrocarbons composed of molecule  $\chi$ . The clustering is necessary to make units large enough so as to produce the well known interstellar scattering and reddening curves. We also showed experimentally that all the interstellar "mini-molecules" such as formaldehyde, ammonia, and water as well as CN and OH radicals, can be made to attach to molecule  $\chi$  and presumably play a role in weakly-bonded clusters of molecule  $\chi$ . Complexing of  $\chi$  molecules, via water molecules has been definitely established spectroscopically. Finally, the total amount of data obtained was so immense that it was not possible to reduce all the data and incorporate it in this report. It is hoped that in the follow-on program, reduction of the low temperature data will be

---

\* In a book entitled "Use of Space Systems for Planetary Geology and Geophysics, Vol. 17, pp 51-66, edited by R. D. Enzmann, published by AAS Science and Technology Series, Tarzana, California.



possible. Also, the survey data has been of immense magnitude since it was important to demonstrate that virtually none of the possible hydrocarbons and porphyrins were omitted for consideration and examination.

With hindsight, most of this spectral survey work is now really of negative interest only (e.g., it proves that no simple hydrocarbon can give the interstellar diffuse lines); consequently, instead of reproducing this vast amount of material, representative data are given. This is done in Section 2. One exception to the above comment is to be noted: more detailed UV and IR interstellar spectroscopy would presumably discover other stable molecular structures in the interstellar medium such as benzene and pyridine which do not have absorption lines in the visible.

#### 1.4 EXPERIMENTAL APPROACH LEADING TOWARDS THE IDENTIFICATION OF MOLECULE X

Before the data is discussed in detail, the techniques and samples employed will be outlined, essentially in the sequence in which the experiments were performed. It may be of historical interest to show the steps leading towards the final solution in the identification. In any event, the large amount of absorption data on porphyrins obtained in this program is not available in the literature under the condition employed in these experiments and hence the porphyrin compilation, in addition to being of use in firmly ruling out a large selection of compounds, will provide a basis for later theoretical analyses of spectroscopic data. Note that the first seven steps were a necessary preliminary to the program plan and may be omitted on first reading.

##### 1.4.1 THE EXPERIMENTAL PLAN

1. Aromatic Hydrocarbons--Perylene, Anthracene, Pyrene, etc. (see Table IV).

2. Nitrogen Aromatics--Carbazole, Indole.
3. Porphyrins--Porphin, Deuteroporphyrin, Haemin, Chlorophyll, Cytochrome, etc. (see Table V).
4. Solid Particle Suspension Spectra.
5. Admixture of Minerals, including carbonaceous chondrite meteorite powder.
6. Temperature effects  $77^{\circ}\text{K} \rightarrow 298^{\circ}\text{K}$  for compounds 1 to 5.
7. Detailed studies on special group of porphyrins--Matrix Suspension (Technique A).
8. The Tetrabenzoporphins:  $\text{H}_2$ , Zn, Fe, and Mg complexes.  
The Pthalocyanines: FePc, MgPc,  $\text{H}_2\text{Pc}$ .  
The Tetraphenylporphins: TPP, MgTPP, FeTPP.
  - a. Effects of solvents.
  - b. Molecular admixtures bonded perpendicular to basal plane.
  - c. Powder matrix suspension vs. liquid suspension.
  - d. Temperature effects (room vs  $77^{\circ}\text{K}$ ).
  - e. Chemical isolation matrix techniques (Shpol'skii)--(Technique B).
  - f. Special spectrometric equipment constructed to measure low intensity transmission data with high precision wavelength determination capability.
    - (1) Scanning spectrometer--lock-in detection, high intensity light source.
    - (2) Photographic--densitometer read-out.
9. Final data runs using techniques of f.(1) and f.(2) on MgTBP in a host of different matrixes and concentrations (Technique B).
10. Comprehensive data runs on pyridine complexes of MgTBP (Molecule X).
11. Study of molecular X clusters--simulation of interstellar reddening curve.
12. Complexing of X molecules with
  - a.  $\text{H}_2\text{O}$
  - b.  $\text{NH}_3$
  - c.  $\text{H}_2\text{CO}$
  - d. CN

13. High sensitivity, low temperature data of X molecules in absorption and emission.
14. IR measurements.
15. Reduction of data.
16. Spectroscopic molecular X vapor data at 500-600°C.
17. Thermodynamic and chemical stability--sublimation tests.
18. Other tests on porphyrin molecules
  - a. Fluorescence measurements
  - b. MCD measurements (preliminary)

### 1.5 ACKNOWLEDGEMENTS

It is a pleasure to thank Dr. Gordon W. Hodgson, Dr. George H. Herbig and Dr. C. E. Castro for many stimulating discussions and insights into each of their respective specialties, carbonaceous meteorites and porphyrins, astronomical data, and the chemistry of porphyrins.

In addition, each provided critically needed help, without which this phase of the project could not have been so speedily completed. Dr. Herbig kindly provided his latest measurements on the diffuse interstellar lines, Dr. Hodgson provided many rare samples of carbonaceous meteorites and selected hydrocarbons, while Dr. Castro provided almost all of the porphyrins, and synthesized the family of TBP Compounds. The generosity of all the chemists too numerous to mention, who so kindly supplied some of the porphyrins is hereby gratefully acknowledged. Dr. G. A. H. Walker kindly forwarded a manuscript prior to publication.

Mr. Dennis Marines provided skilled assistance with the laboratory measurements throughout the program. Mr. S. Dobrin assisted in the measurements during the summer of 1969.

The support and encouragement by Mr. Maurice Dubin of NASA Headquarters is gratefully acknowledged.

## SECTION 2

### EXPERIMENTAL RESULTS

#### 2.1 DESCRIPTION OF EQUIPMENT AND TECHNIQUES

Three basic matrix techniques were used to investigate absorption at the 77°K. The first, involving frozen glasses such as EPA was used only in the first phase, three years ago. It was abandoned because of the strong interactions of the matrix with the dissolved molecules. The second technique, A, was explored in depth, it consisted of pulverizing the chemicals to be studied in an automatic pestle and mortar grinding machine and suspending the particles in a matrix such as silicone grease between two glass slides. The third technique, B, is basically the Shpol'skii technique. It was found to be more of an art than a science to obtain the desired inert matrix suspension. Hence in order to eliminate any possible artifact or systematic errors arising from matrix effects, a very large number of variations, both in chemicals, mixtures and chemical treatment of samples were carried out. Surprisingly, the variations so encountered were less than the quoted precision 1-2%. The only distinct effect arises from drastic changes in the concentration of molecule  $\chi$  indicating that the dominant effect is molecule-molecule interaction. In the extreme case of finely divided  $\chi$  powder, the Soret band broadens, shifts and may even disappear.

The main equipment used on this program was a Beckman DK2 spectrophotometer for survey work from 0.2 to 3.0  $\mu$ . Because of the ease of its operation, all samples were first examined on this instrument before



more detailed studies were undertaken. Precision measurements required two different techniques (see Fig. 2). Either a system comprising phase sensitive detection using a 1/2m Jarrell Ash scanning spectrometer, a very intense light source (300 watts tungsten or a high pressure arc lamp), a sensitive S20 photomultiplier and recorder; or in place of the electronics a 3/4m photographic Jarrell Ash spectrometer. The latter technique corresponds closest to the actual astronomical method of observing the diffuse interstellar lines.

Superimposed on the absorption spectrum were standard reference spectra, to enable subsequent precision wavelength determinations on a scanning spectrophotometer. Wavelength determination should be accurate to  $\pm 1\text{\AA}$ . The samples were placed in a cell inside a specially constructed dewar (described in the previous final report, 1967). Care was taken in the freeze down procedure. Generally, best results were obtained by very slow cooling procedures. The red fluorescence characteristic of molecule  $\chi$  was always very conspicuous. Photographs showing the basic equipment are seen in Fig. 3 and 4.

## 2.2 SUMMARY OF LOW TEMPERATURE MATRIX ISOLATION DATA - (TECHNIQUE A)

Two completely different techniques were used in the spectroscopic low temperature matrix isolation measurements. In Technique A, we attempted to simulate interstellar dust grains according to the ideas of Van de Hulst and others who assumed these grains were of a certain size distribution (in the micron range) with possible admixtures of atoms or molecules which would give rise to the hitherto unidentified diffuse interstellar absorption lines. We exhaustively surveyed a large selection of polycyclic aromatic compounds including porphyrins, nitrogen aromatics, admixtures of minerals, by grinding these chemicals into a fine powder and embedding them in a solid matrix of silicone grease.

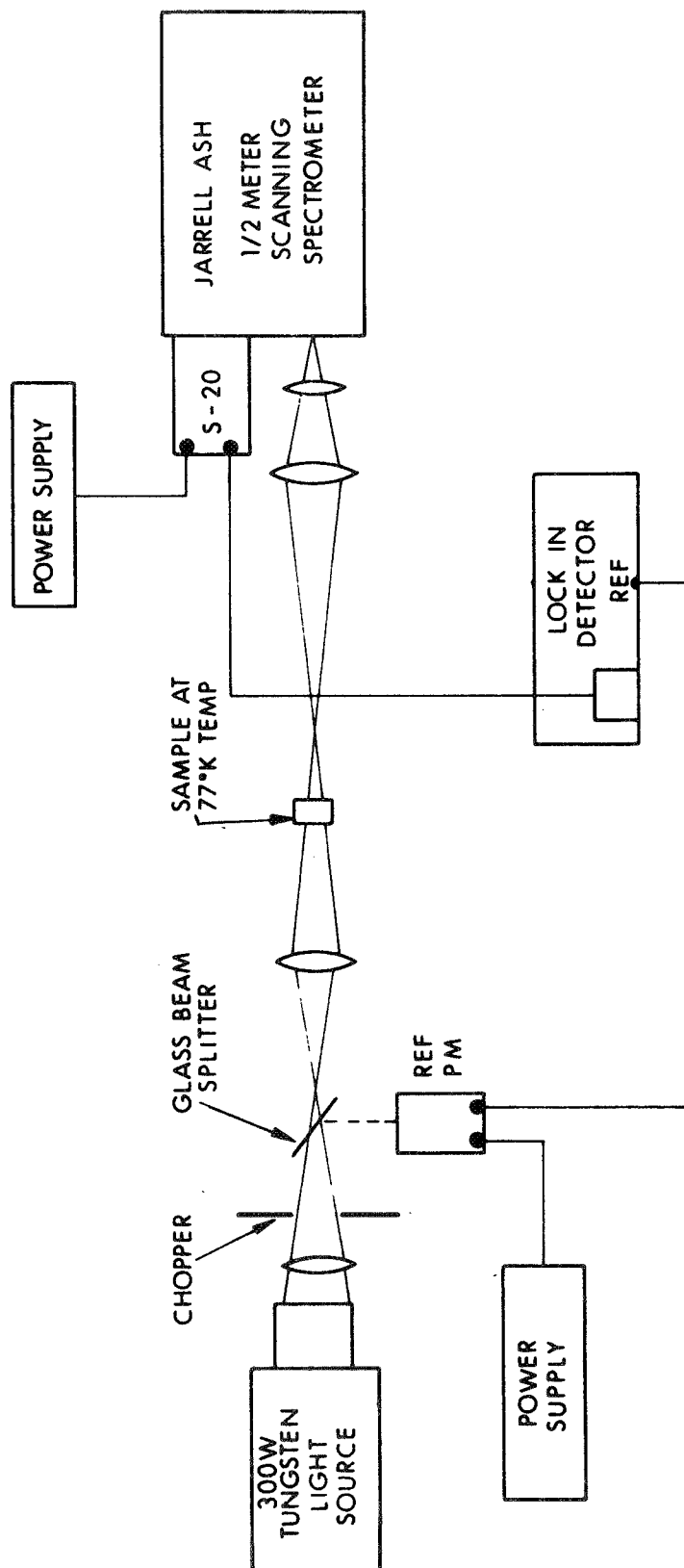


Figure 2. Schematic Diagram of Experimental Arrangement

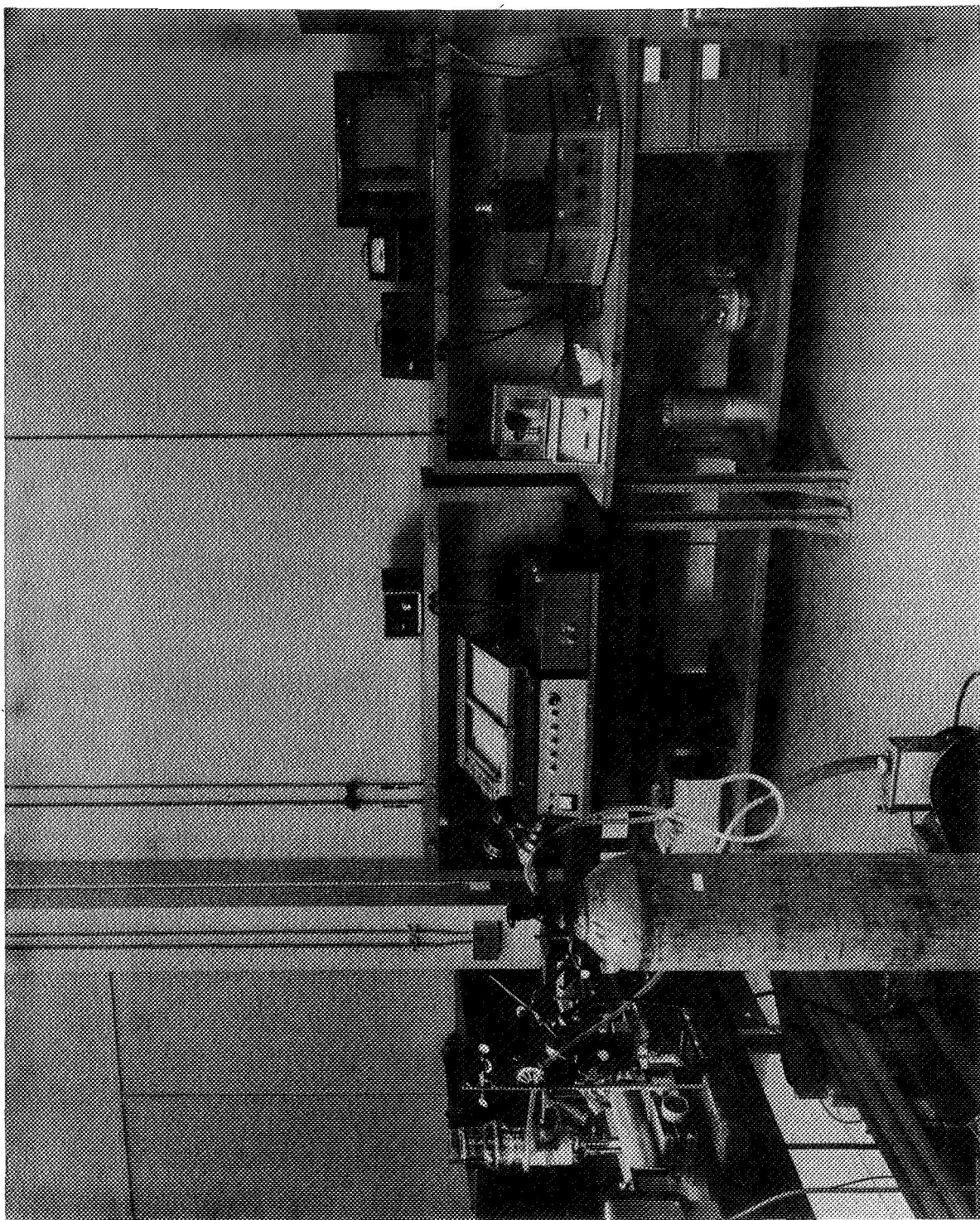


Figure 3. Photograph of Experimental Equipment Showing Overall Layout.  
Beckman Spectrophotometer and Automatic Mortar Grinding  
Equipment May Be Seen in the Background.

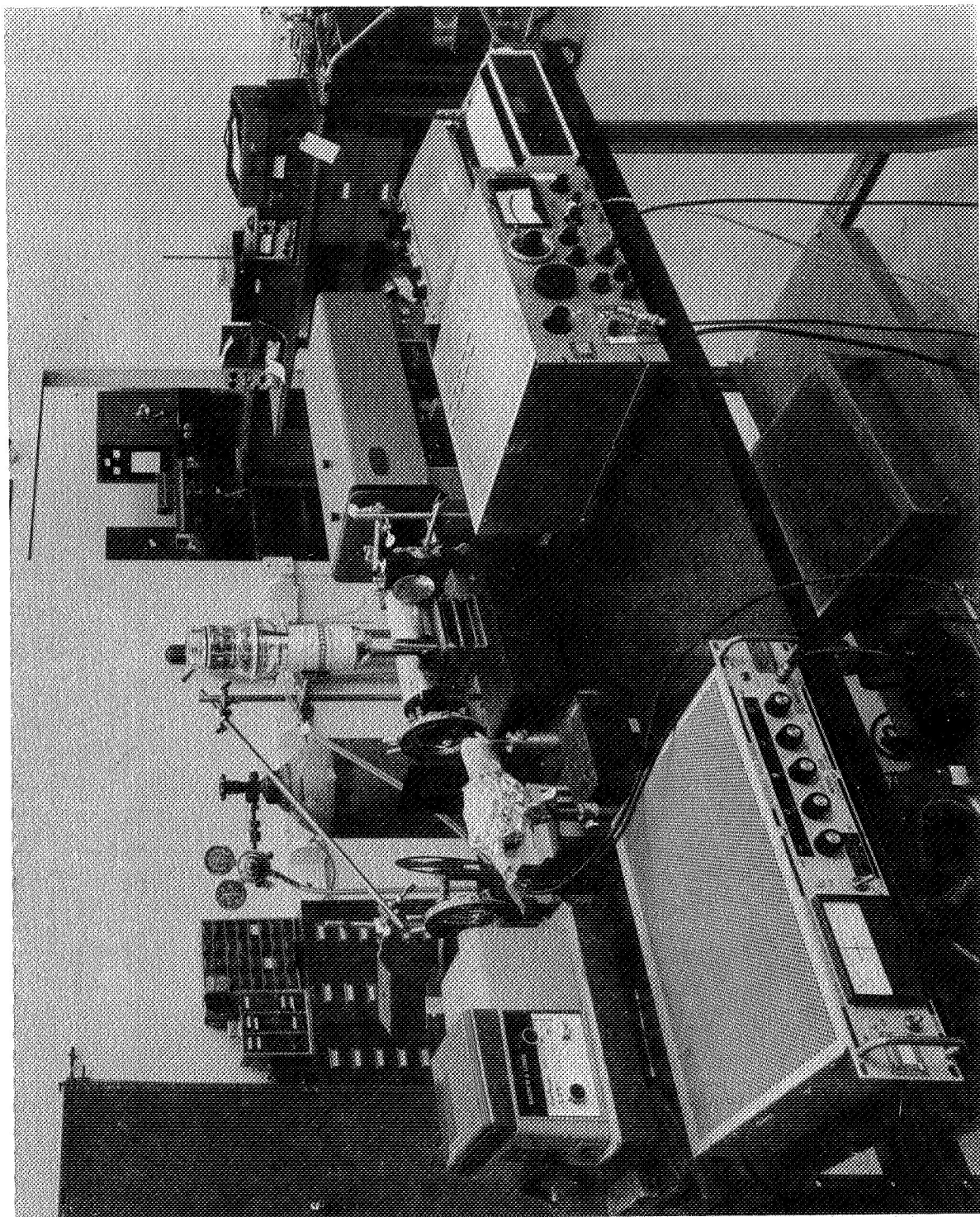


Figure 4. Photograph of Experimental Equipment. Following details are shown: sensitive photodetection equipment showing light source, dewar, scanning spectrophotometer, lock-in detector, and strip-chart recorder.



The compounds porphin and perylene were used as prototypes to study the effects of solution and matrix suspension. Tables I and II summarize the data obtained by using two solvents, namely chloroform and ether, and compare these data with a fine powder suspension using grease as the matrix. The samples were examined first at room temperature and then at liquid nitrogen ( $\text{LN}_2$ ) temperature in a fine powder matrix suspension. Various additive compounds, including chalk, alumina powder, and even toothpaste, were used to enhance the lines and cause multiple scattering. The effects of these additives have to be watched chemically, since the important Soret band is strongly affected by some of these compounds, and in fact vanishes for chalk and toothpaste. It is possible to follow the intensity of the wavelength maxima and the overall intensity distribution of the bands. It should be pointed out that the wavelength shift is generally about  $100\text{\AA}$  (greater for perylene) to the longer wavelength for the samples in fine matrix suspension at  $\text{LN}_2$  temperatures. The effect of temperature apparently is not as great as that of the means of suspension, since the intensity maxima of the fine powder suspension data do not vary too greatly between room temperature and  $\text{LN}_2$  temperature. However, the shape of the curves and the general spectra are significantly different comparing the room temperature with the  $\text{LN}_2$  temperature data. Considerable sharpening of the lines occurs as the sample is cooled to  $\text{LN}_2$  temperature. Thus, we can conclude that mixtures of silicate and carbonate minerals generally weaken the absorption spectra of organic compounds, and in some cases cause the Soret band to vanish almost completely.

Data taken for perylene and porphin mixtures with admixtures of a finely divided powder of the carbonaceous chondrite Murray caused spectra to be observed which very closely simulated the interstellar scattering curve with the small superposition of absorption lines at  $4400\text{\AA}$  and  $4700\text{\AA}$ .

TABLE I  
PORPHIN ABSORPTION MAXIMA

<u>Temp.</u>	<u>Solvent/ Additive</u>	<u>Soret</u>	<u>IV</u>	<u>III</u>	<u>IIa</u>	<u>IIb</u>	<u>I</u>
Room	chloroform	3900	4860	5150 (5500)	5580	5650	6100
Room	ether	( $\approx$ 3900)	4845	5120	5590	5650	6145
Room	grease	4045 shallow	5085 broad		5725 broad		6200 enhanced relative to other bands
77°K	grease	3745 shallow	5125 shallow	5450	5700 sharp weak	5790	6250
77°K	toothpaste	gone	5050	5275 (5670)	5675	5750	6205
77°K	toothpaste	gone	5050	5355	5660 sharp	5725	6215
77°K	grease + chalk	3900 weak shallow	5050	5370	5670	5735	6205
77°K	grease + alumina	3940 strong sharp 100Å wide	5115 weak		5650	5725	6195
77°K	50% porphin 50% shale	3940 very shallow 600Å wide	5195 very shallow	5435 very weak (5575)	5675 sharpest line	5745 very weak	6225

TABLE II

## PERYLENE ABSORPTION MAXIMA

<u>Temp.</u>	<u>Solvent/ Medium</u>	<u>Mixture</u>	<u>Strongest</u>	
			<u>Line</u>	<u>Line</u>
Room	chloroform	3700	3875	4100
				4370
				4850
				5575
Room	grease		4000	4290
77°K	grease			4600
				4725
77°K		50% Murray		4400
				4700
				4375
				4610
77°K		Murray + perylene		
				5675, 6200
				5740

excellent spectra  
simulating scatter-  
ing curve of inter-  
stellar dust.

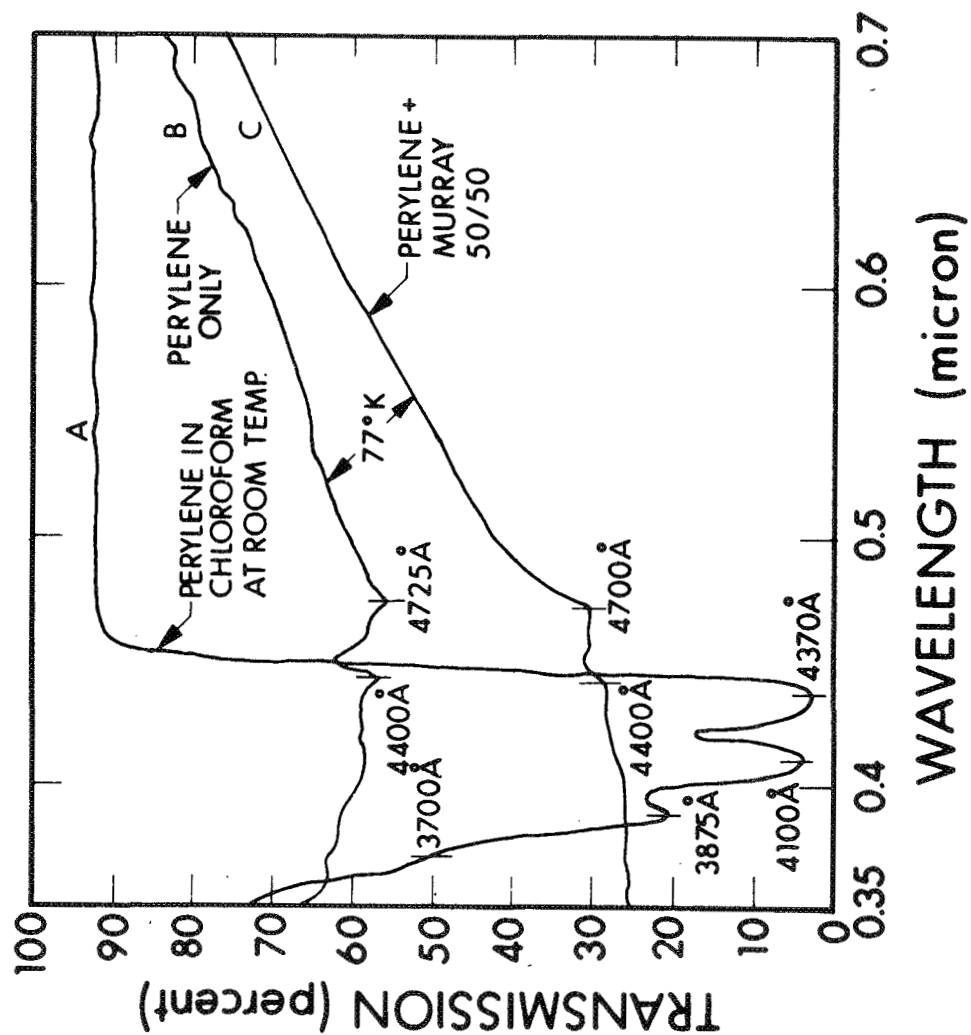


Figure 5. Solution Data Compared with Powder Matrixes at 77°K

Figure 5 compares data taken of perylene in liquid solution at room temperature (curve A) and in a powder matrix at  $\text{LN}_2$  temperature (curve B). Curve C shows data for a mixture of perylene and Murray. Table 1 shows the same data for porphin at a temperature of  $77^\circ\text{K}$ . The composition spectra were suggestive of the type of spectra one would anticipate for the interstellar dust in terms of scattering as a function of wavelength and the superimposed absorption features.

A set of 18 porphyrin compounds were specially prepared by our chemical consultant, Dr. Castro. The spectra of these compounds were studied exhaustively under matrix suspension technique A at  $77^\circ\text{K}$ . The results of three such runs are shown in Figs. 6 and 7. Photographs were taken of the various matrix suspensions showing the particle size distribution (Figs. 8, 9 and 10). The scale at the top of the photograph permits determination of the particle sizes.

It was found that admixtures of compounds play an important role in enhancing the absorption effects, presumably by increasing the optical path lengths via multiple scattering centers. Another interesting observation that can be ascertained from Figs. 6 and 7 is the association of both absorption and dispersion with the asymmetric line shapes; that is, because of the Kramer-Konig relationships, an obvious dependence exists between these two effects.\* The interstellar diffuse absorption lines are indicated below the experimental data to show how very strongly suggestive some of the preliminary results were at that time (Fig. 6). The precision, however, was totally inadequate at that point to make any identification. Moreover, the results were merely suggestive and encouraging for further search. Thus the search for the elusive porphyrin went on.

---

\*See discussion on Reddening (Section 3.7)

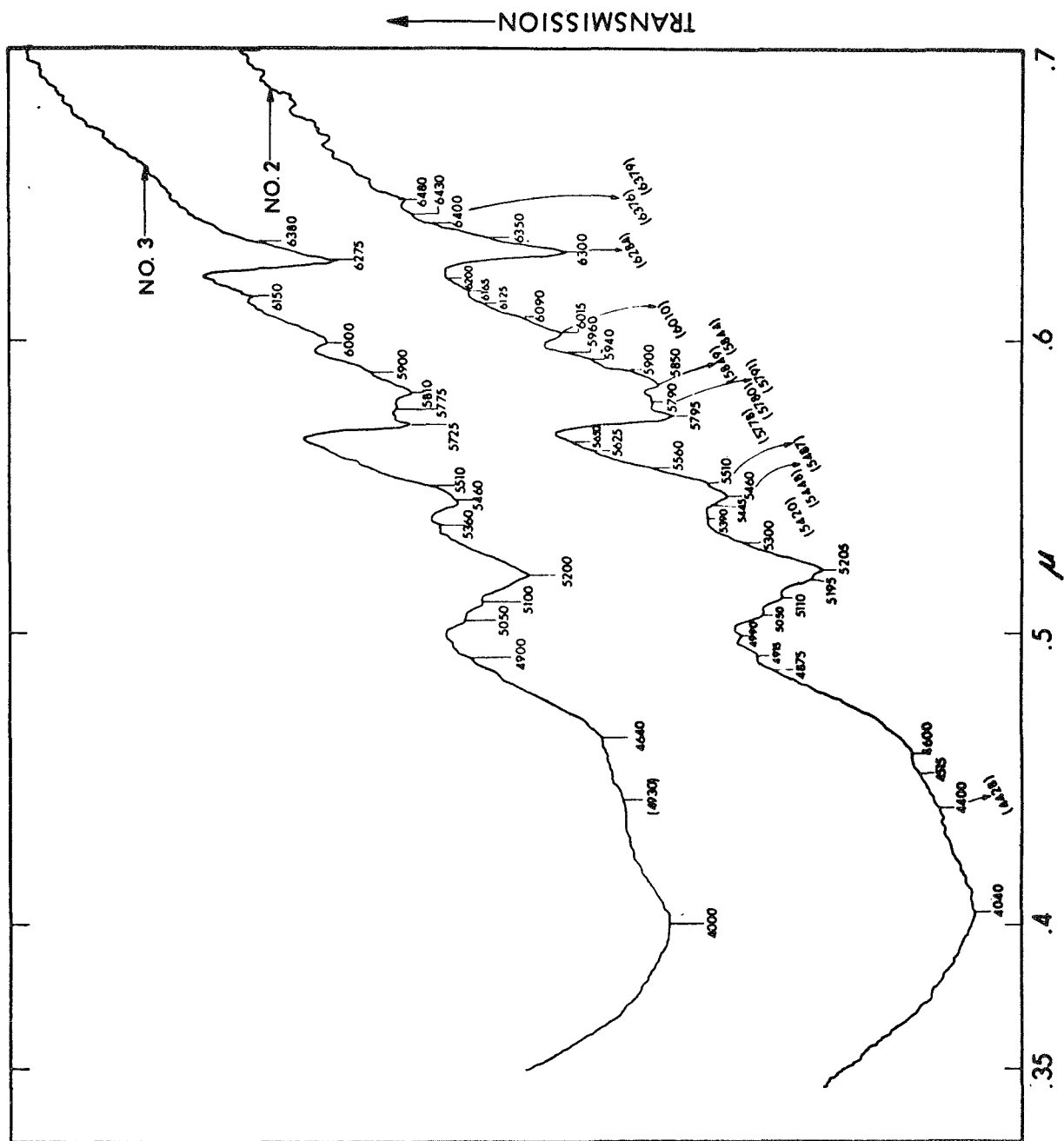


Figure 6. Prophyrin Powder Suspensions (Technique A)

OT-9-9506

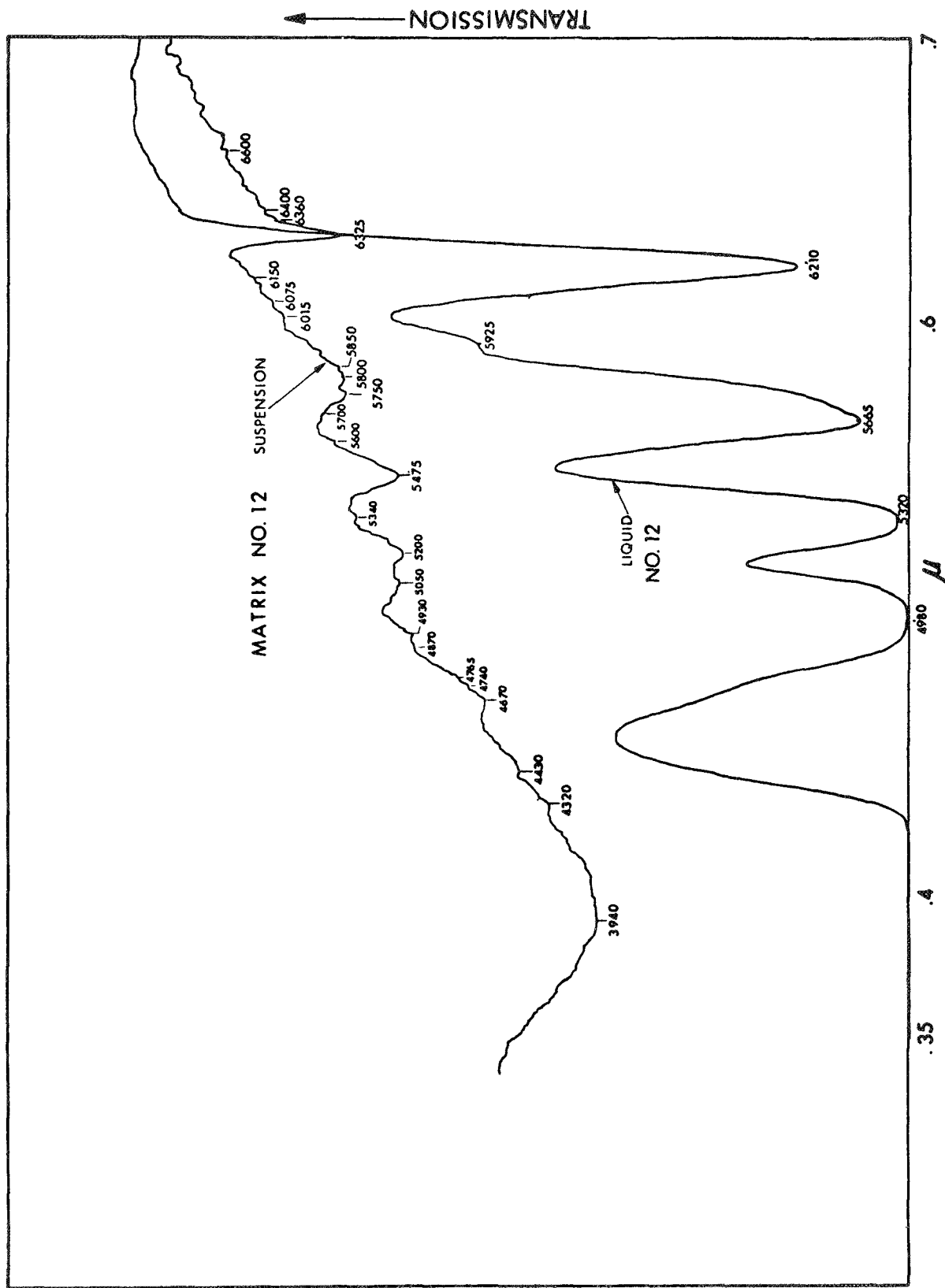


Figure 7. Powder versus Liquid Suspension

01-9-9505

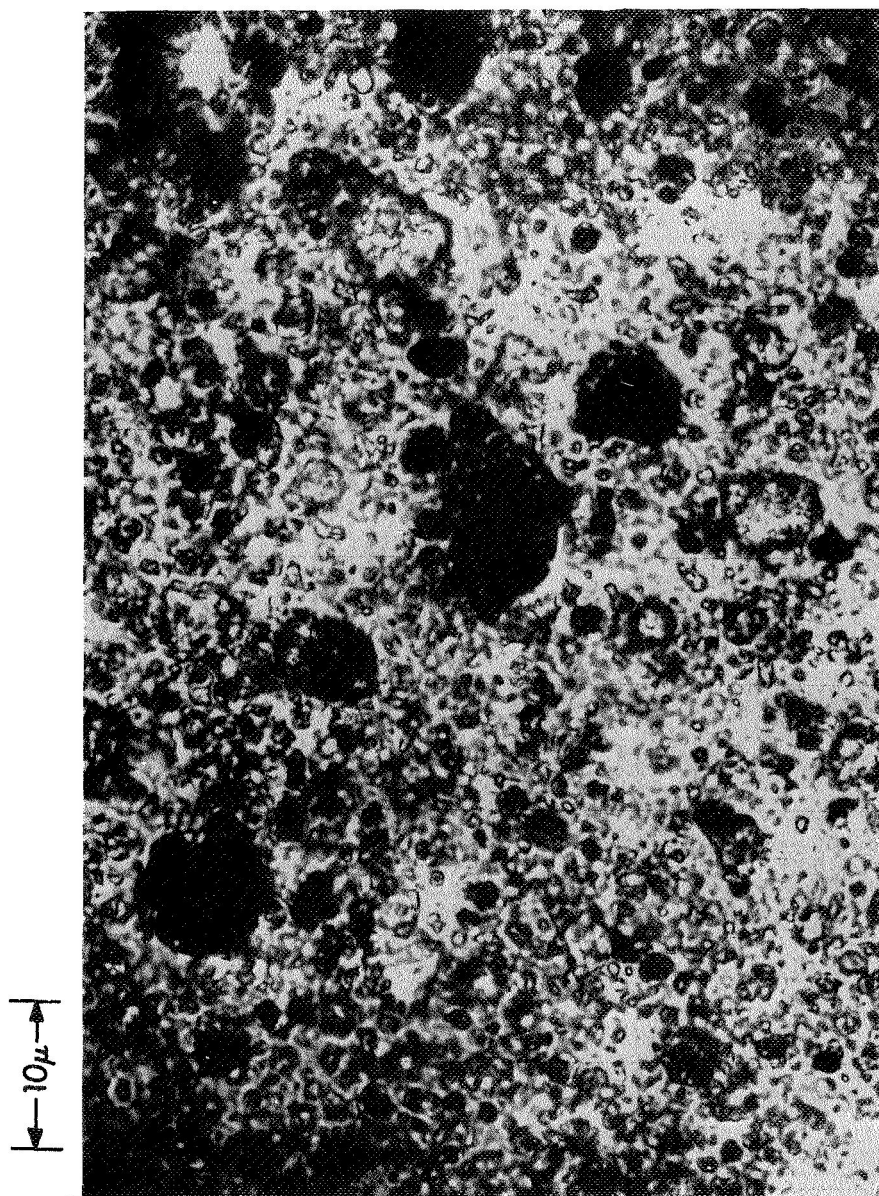


Figure 8. Microscope Photograph Enlargement of Specimen Containing  
Admixture of Porphyrin + Perylene + Murray



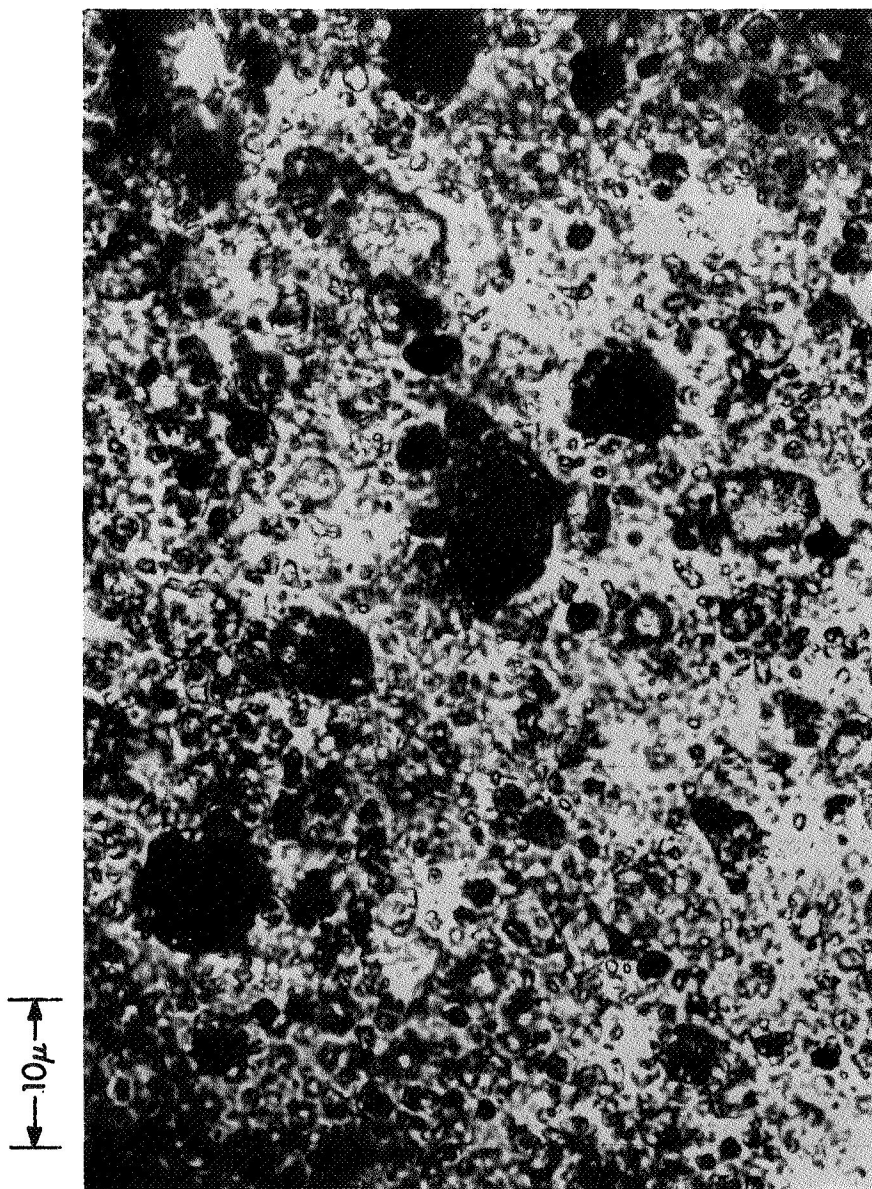


Figure 9. Microscope Photograph Enlargement of Specimen Containing  
Admixture of Perylene + Murray

100  $\mu$

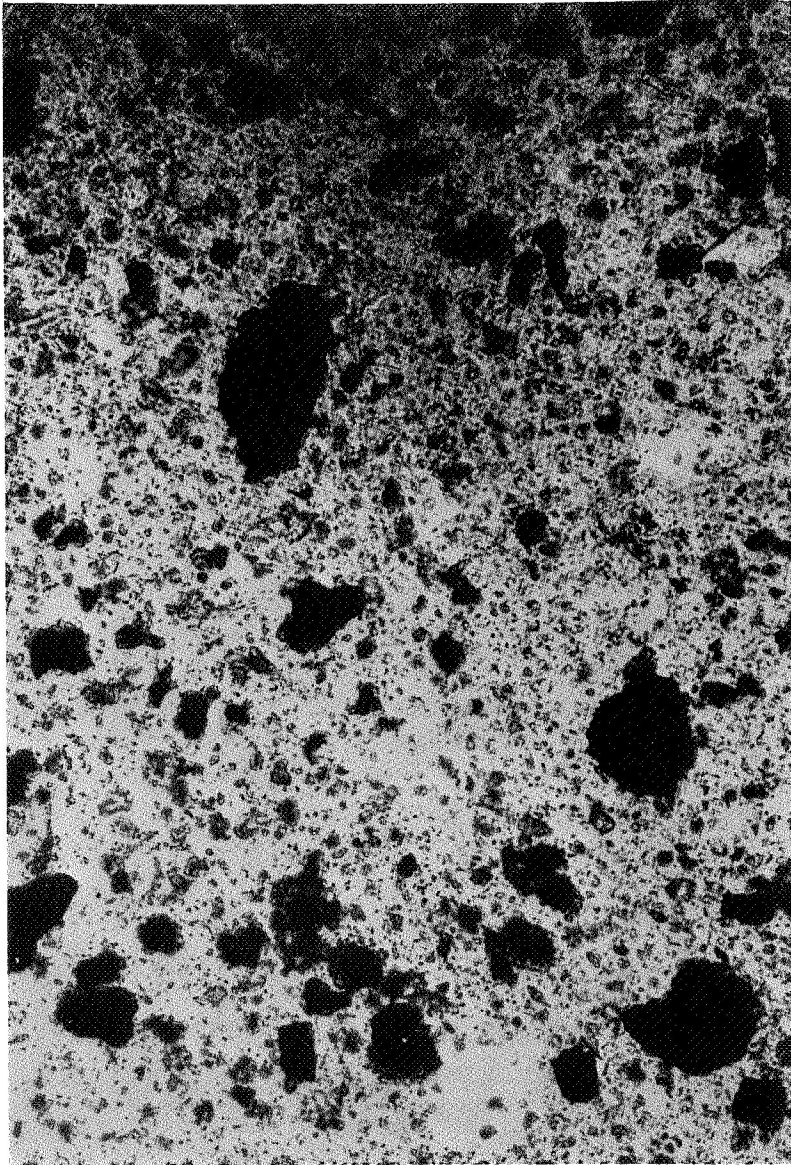


Figure 10. Microscope Photograph Enlargement of Specimen Containing  
Admixture of Sample No. 2 with Meteorite Powder from  
Orgueil

# TABLE III

## PORPHYRIN COMPOUNDS STUDIED

### Set A

1. Hematoporphyrin
2. 2,4-Di(alpha-thiophenylethyl)deuteroporphyrin dimethyl ester
3. 2,4-Di(alpha-thiophenylethyl)deuteroporphyrin
4. Deuterohemim dimethyl ester
5. 2,4-Di(alpha-thiophenylethyl)deuterohemim dimethyl ester
6. Deuterohemim (chloride)
7. Protohemim (IX)
8. Protoporphyrin
9. Protohemim dimethyl ester
10. 2,4-Di(alpha bromoethyl)deuteroporphyrin
11. octamethylporphyrin
12. octaethylporphyrin
13. octaethylhemim
14. Iron(II) Phthalocyanine
15. Iron(II) Phthalocyanine Diquinoline
16. Mesoporphyrin (IX)
17. Mesohemim (IX) dimethyl ester
18. Phthalocyanine Iron (II) (III)

### Set B

- 19 - 22  $H_2$ ,  $Z_n$ , Mg, Fe Tetrabenzporphines
- 23 - 26 Cu,  $H_2$ , Mg, Fe Pthalocyanines
- 27 - 29  $H_2$ , Mg, Fe Tetraphenylporphins
30.  $\chi$  (MgTBP) + pyridine
- 31 - 34  $\chi$  + Additives:  $H_2O$ ,  $H_2CO$ ,  $NH_3$ , CN

## 2.4 DETAILED DISCUSSION OF RESULTS USING TECHNIQUE A<sup>\*\*</sup>

### 2.4.1 CHEMICAL STRUCTURE

#### 2.4.1.1 Aromatic Compounds

About fifty aromatic hydrocarbons of increasing complexity were examined in the present study. As shown in Table IV they ranged from simple coupling of benzene rings to massive fusing of such rings into graphite-like molecules of six rings and more. As a general rule, the larger the number of condensed rings in a compound, the longer the wavelength of its initial absorption bands. For example, benzene absorbs strongly in the ultraviolet, with its initial band at about 280 nm. Pentacyclic perylene has its initial band at about 432 nm. The foregoing data are for the compounds in solution at room temperature.

In the solid state, however, the absorption bands are superimposed upon a scattering background of considerable intensity depending on the dispersion of the solid organic matter. The peaks of perylene as shown in Fig. 5 are broadened from band widths of about 10 nm to about 25 nm, and in addition they are shifted to longer wavelengths by about 35nm.

#### 2.4.1.2 Aromatic Compounds With Hetero Atoms

Nitrogen-containing aromatic compounds showed similar effects. The compounds studied were indole, carbazole, dibenzocarbazole, benzoquinoline, phenazine and benzonitrile. Carbazole for example, showed peak broadening of about 50%; peak shift was 15 nm to the red.

---

<sup>\*\*</sup> The contributions by Dr. G. W. Hodgson to the discussion in Section 2.4 are gratefully acknowledged.

Oxygen analogs were dibenzofuran and 2, 3-benzodiphenylene oxide, and the same effects were observed.

#### 2.4.1.3 Nitrogen-containing Dyes\*

To test the effects due to azo-nitrogen bonding, the following dyes were examined: Methyl Red, Brilliant Green, Bismark Brown and Auromine O. All of the dyes show broad bands in aqueous solution with band widths in the range of 80-150 nm. In the solid state the absorption bands become too broad to be discerned.

#### 2.4.1.4 Sulfur Compounds\*

Phosphorous pentasulfide exhibits three bands in the blue end of the visible spectrum. In solution (benzene-methanol) these occur at 450, 425 and 400 nm. The most intense band (450 nm) has a band width of about 5 nm. In the solid state this compound gives a spectrum yet to be determined.

The phenomenon of the formation of polysulfides through addition of elemental sulfur to sulfides is well known. For example sulfur adds to sodium sulfide giving an intense yellow chromophore at 408 nm with a band width of about 40 nm. In the solid state sodium polysulfide behaves in a manner yet unknown to us.

#### 2.4.1.5 Porphyrins

Eighteen porphyrins of varying structural configurations were examined. These are illustrated in Table V and range from unsubstituted porphin to highly substituted hematoporphyrins. In solution porphyrins have

---

\* This data was kindly supplied by Dr. G. W. Hodgson.

an intense band near 400 nm and several less intense bands in the red end of the spectrum. When examined in the solid state porphyrins showed a strongly modified pattern in which the major (Soret) band is weakened and broadened to a marked degree. The non-Soret bands, however, remain clearly discernible and are shifted to longer wavelengths by about 5-15 nm. While some broadening of the non-Soret bands is evident, it seems quite limited. Figure 6 or 7 illustrates this change in spectrum for two porphyrins. Again as with the other organic compounds, the background due to scattering is clearly evident, increasing with shorter wavelengths.

#### 2.4.2 TEMPERATURE EFFECTS

Two manifestations of temperature change are considered. In one, there is a phase change with decreasing temperature, with, for example, a change from the liquid state to solid state. In a sense the foregoing data have dealt with this kind of temperature change involving changes from solution state to crystalline solid state for the organic compounds.

Figure 11 presents the change experienced when ovalene--a ten-ring aromatic hydrocarbon--was cooled from room temperature to 77°K. A shift of about 6 nm to longer wavelength is noted for the initial absorption band, and in addition a clear-cut sharpening of the individual bands is evident. The sharpening was about 25% reduction in band width, i.e., from 15 to 11 nm.

#### 2.4.3 MATRIX EFFECT (TECHNIQUE A)

The foregoing results were obtained without regard to the detailed physical state of the organic matter. In general, the organic compounds were obtained in crystalline form and ground in a mortar to a particle size less than 0.2 mm in diameter. The powdered solid was then suspended in the light path of the spectrophotometer by sandwiching it

between two optical faces either alone or with an inert binder, Dow Corning silicone stopcock grease. In nearly all instances, the spectrum obtained for the dry powder was indistinguishable from that for the suspension in silicone grease. Accordingly, the grease matrix was used as a matter of convenience, except in those rare instances wherein the organic compound under examination was slightly soluble in the silicone preparation giving rise to a regular solution-type spectrum.

In some experiments, water was added to test its effect on the absorption character of the organic compounds. Except in the case of nitrogen-containing dyes that were soluble in water, the only noticeable effect was to reduce the background scatter.

To more closely approach the "presumed"\* interstellar conditions involving the presence of inert inorganic substances, many experiments were carried out with admixtures of known mineral substances. In the first instances, this was done by grinding the organic and inorganic substances together with silicone grease in the mortar. The solids comprised silica gel, alumina, glass, carbonates, shales and carbonaceous chondrites (Orgueil, Murray and Pueblito de Allende). The general effect in nearly all cases was for the inert solids to merely dilute the absorption of light by the organic substances. In some instances the organic compounds still showed discernible spectral features at concentrations of a few percent of the total aggregate.

In some instances, moreover, the presence of particular inert solids seemed to enhance the absorption features of the organic compounds. This was evident primarily in experiments involving admixtures with silica gel, alumina and glass powders. Silica gel and alumina particles strongly adsorb organic substances on their surfaces; glass of course, is more transparent than other mineral aggregates. Consequently, further attention was directed to the absorptive characteristics of

\*This was written prior to  $\chi$  identification.

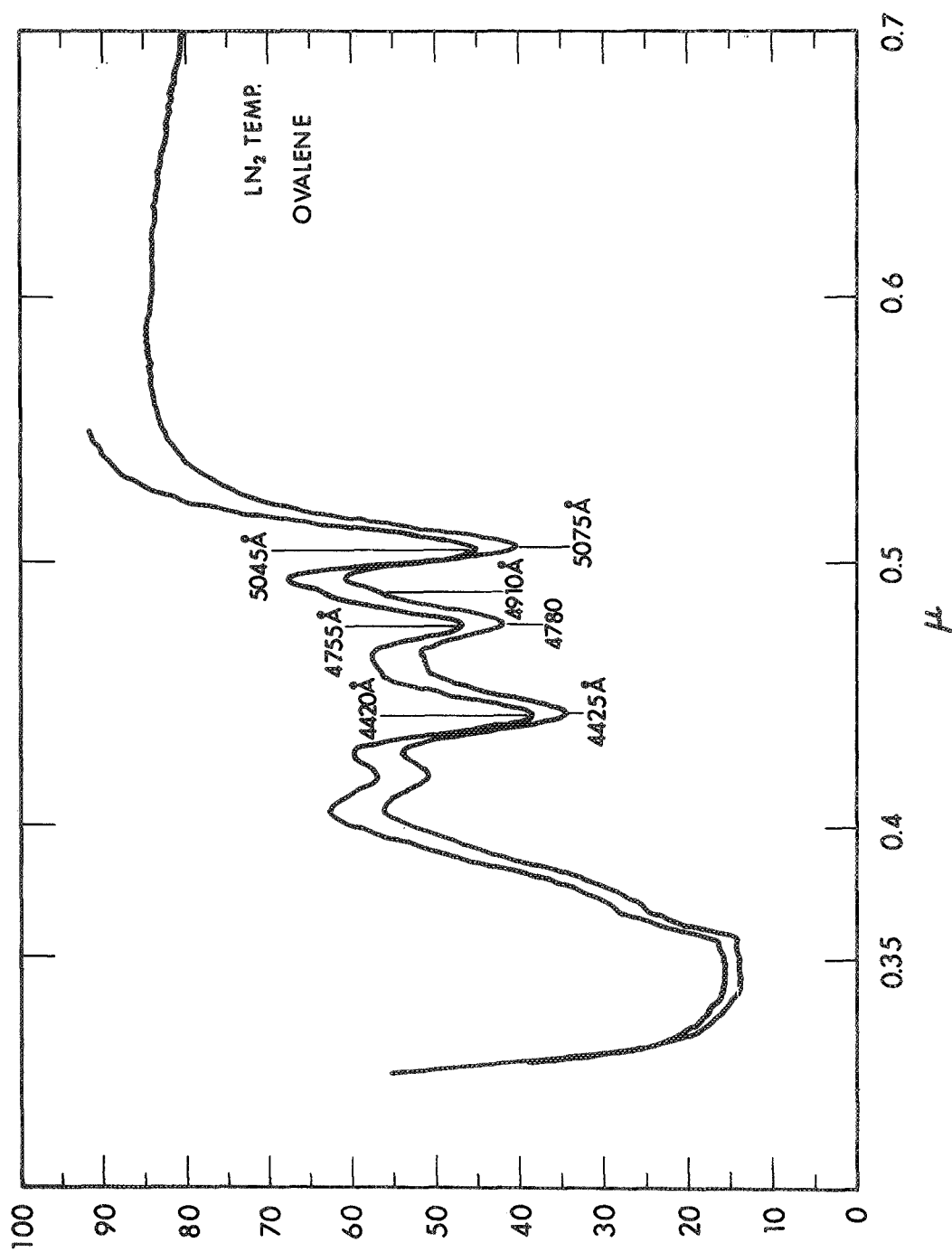


Figure 11. Absorption Spectra of Ovalene at 77°K (Technique A)



organic compounds of primary interest on the surfaces of such solids. In detail, the experimental approach was as follows. Mesoporphyrin IX dimethyl ester was dissolved in benzene to give a saturated solution. A few microliters of the solution were placed on a flat optical face and the solvent allowed to evaporate. The resulting film showed a weak rounded Soret band but distinct non Soret bands. The same solution evaporated onto finely-divided sodium carbonate and silic acid powders gave no discernible absorption features. The same procedure for chromatographic silica gel gave well defined spectra as in the case of the evaporated film, but similar concentrations on the same silica gel, reduced to a very fine powder, failed to give any significant features. Glass spheres embodying the surface effect of a flat optical surface while retaining the particulate aspect of presumed interstellar dust, when coated with mesoporphyrin from solution, gave sharp spectra for non-Soret bands; the Soret band was almost completely suppressed. Two sizes of glass beads were used, 0.27 and 1.0mm, and there were no differences in spectra noted. Figures 11, 12, and 13 are representative data for 3 hydrocarbons out of a total of 50 that were studied--see Table IV.

#### 2.4.4 MIXTURE EFFECT

All of the compounds included in the present study, with the exception of porphyrins, exhibited absorption bands at widely scattered positions in the ultraviolet and visible spectrum. With little or no interaction between the compounds, the spectral features of mixtures of these compounds are taken to be simply additive, and the net effect is to give a curve (see Fig. 14) which is characteristic for random mixtures of large numbers of these compounds. Note that it does not show any spectral features from 5000-6600Å. Also the change in slope short of 4880Å is opposite to what is observed astronomically. These experiments have a bearing on recent theoretical discussions by B. Donn\*, who proposed

---

\* B. Donn, Ap. J. Lett., 152, L 129 (1968).

TABLE IV  
EXAMINED HYDROCARBONS


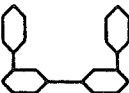
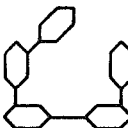

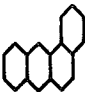
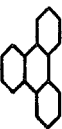
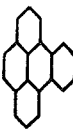



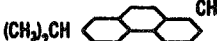
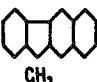
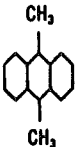

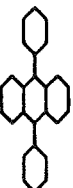
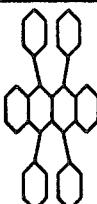
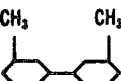
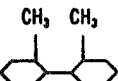
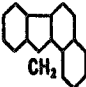
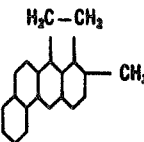
 <p><b>o-QUATERPHENYL</b></p>	 <p><b>m-QUATERPHENYL</b></p>	 <p><b>m-QUINQUEPHENYL</b></p>	 <p><b>PERYLENE</b></p>
 <p><b>1,2-BENZANTHRACENE</b></p>	 <p><b>TRIPHENYLENE</b></p>	 <p><b>1,2-BENZPYRENE</b></p>	 <p><b>3,4-BENZPYRENE</b></p>
 <p><b>p,p'-BITOLYL</b></p>	 <p><b>p-QUINQUEPHENYL</b></p>	 <p><b>RETENE</b></p>	 <p><b>2,3-BENZFLUORENE</b></p>
 <p><b>9,10-DIMETHYL ANTHRACENE</b></p>	 <p><b>CORONENE</b></p>	 <p><b>9,10-DIPHENYL ANTHRACENE</b></p>	 <p><b>RUBRENE</b></p>
 <p><b>m,m'-BITOLYL</b></p>	 <p><b>o,o'-BITOLYL</b></p>	 <p><b>1,2-BENZFLUORENE</b></p>	 <p><b>20-METHYL CHOLANTHRENE</b></p>

TABLE IV (Continued)  
EXAMINED HYDROCARBONS


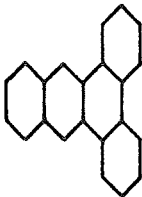

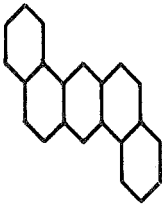
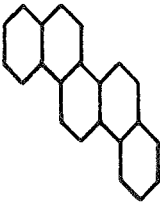
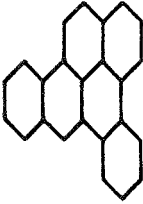
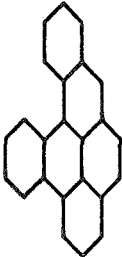

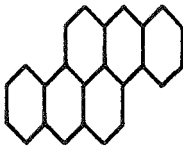
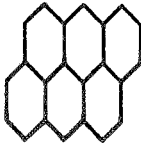
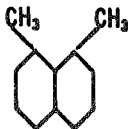
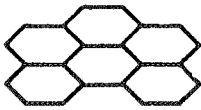



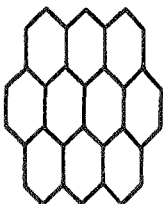

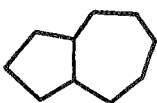

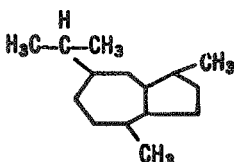


 <p>TRIPTYCENE</p>	 <p>1,2,3,4-DIBENZANTHRACENE</p>	 <p>2,3,6,7-DIBENZANTHRACENE</p>
 <p>1,2,5,6-DIBENZANTHRACENE</p>	 <p>1,2,7,8-DIBENZPHENANTHRENE</p>	 <p>1,2,4,5-DIBENZPYRENE</p>
 <p>1,2,3,4-DIBENZPYRENE</p>	 <p>3,4,9,10-DIBENZPYRENE</p>	 <p>3,4,8,9-DIBENZPYRENE</p>
 <p>ANTHANTHRENE</p>	 <p>1,8-DIMETHYL NAPHTHALENE</p>	 <p>1,12-BENZPERYLENE</p>

TABLE IV (Continued)  
EXAMINED HYDROCARBONS

 <p><b>o-METHYL BIPHENYL</b></p>	 <p><b>m-METHYL BIPHENYL</b></p>	 <p><b>p-METHYL BIPHENYL</b></p>
 <p><b>OVALENE</b></p>	 <p><b>ADAMANTANE</b></p>	 <p><b>AZULENE</b></p>
 <p><b>4, 5-METHYLENE PHENANTHRENE</b></p>	 <p><b>GUAIAZULENE</b></p>	 <p><b>BIPHENYLENE</b></p>
	 <p><b>p-SEXIPHENYL</b></p>	

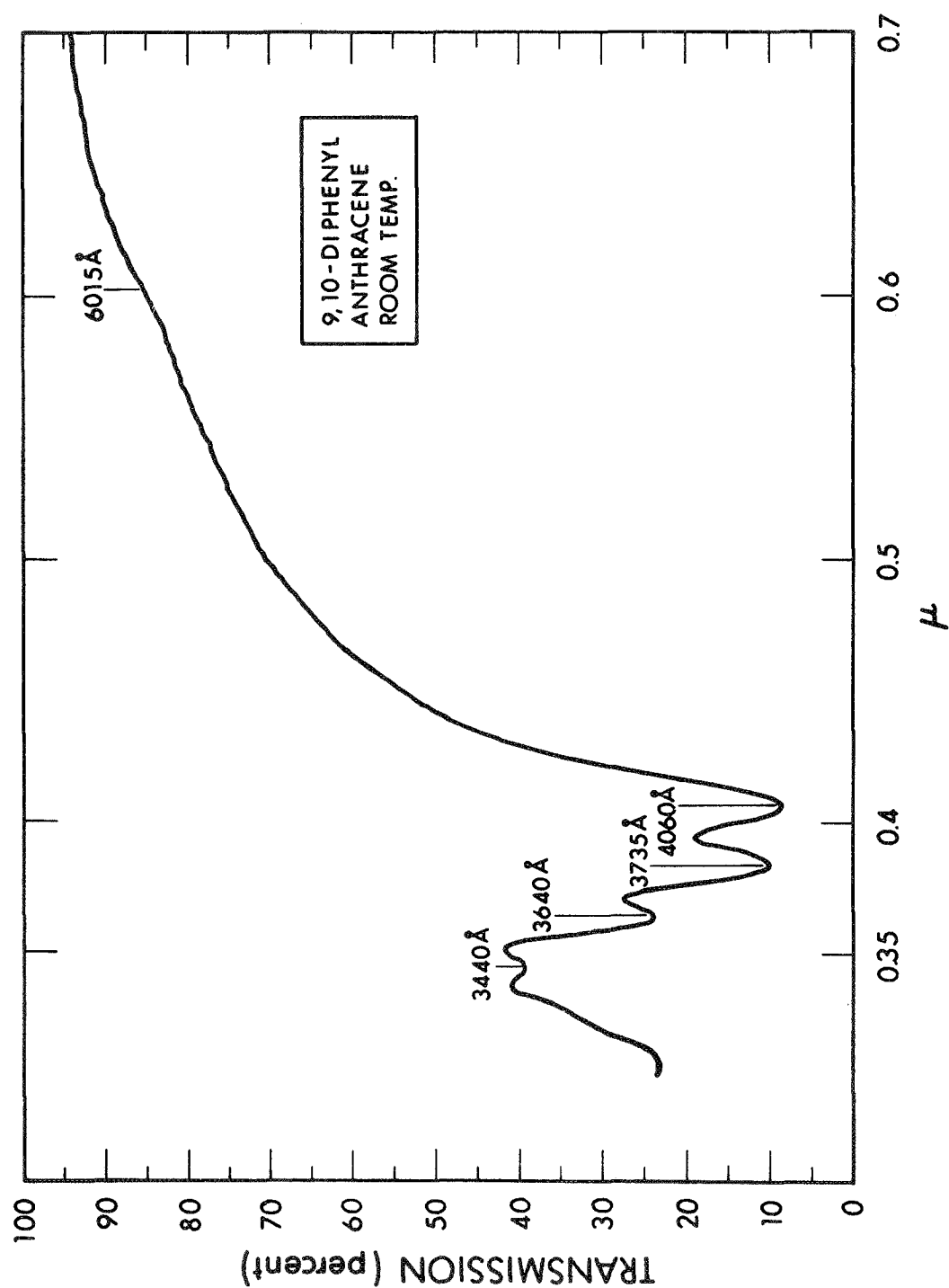


Figure 12. Typical Absorption Spectra (Technique A)

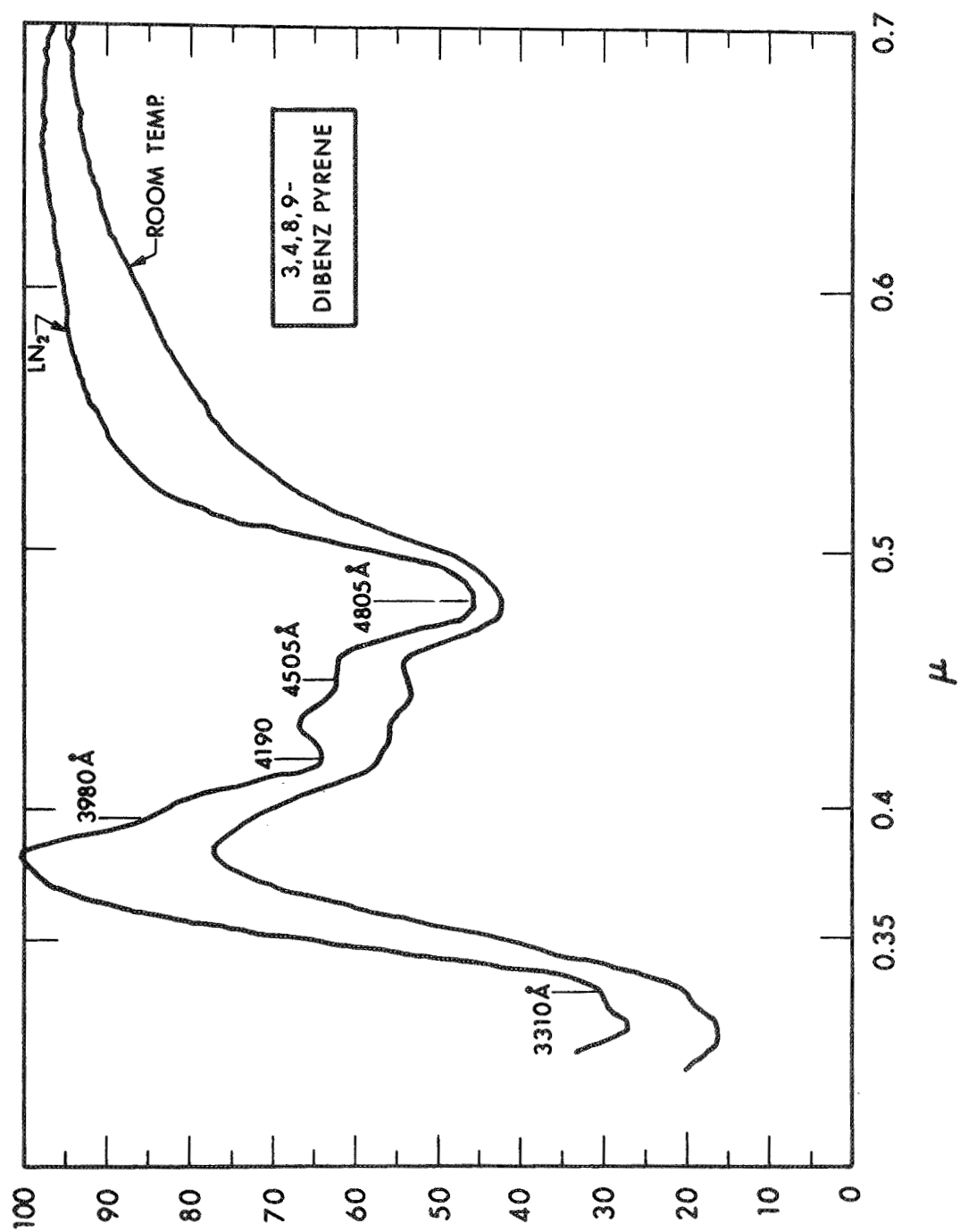


Figure 13. Temperature Effects on Absorption Spectra

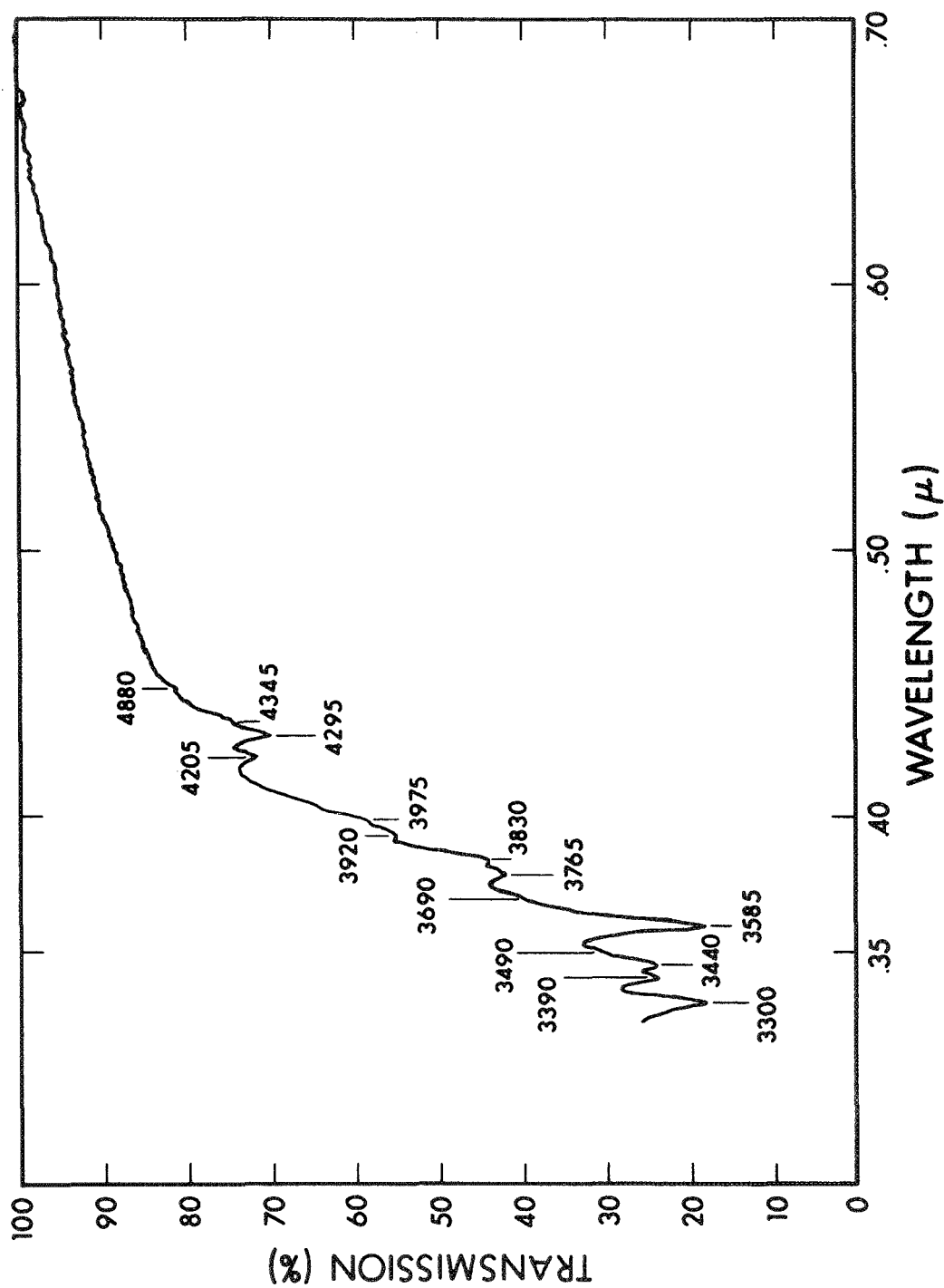


Figure 14. 52 Aromatic Hydrocarbon Composite Spectrum -- in Powder Matrix Suspension (Technique A)

that such a composite mixture might both simulate the wavelength dependence of interstellar extinction as well as reproduce the interstellar lines. (It does not.)

## 2.5 DETAILED RESULTS USING TECHNIQUE A (PORPHYRINS, SET A) AND DISCUSSION

The set of 18 porphyrin compounds of set A (see Table III) provided for us were modified chemically so as to cause various different appendages to be substituted on its basic skeleton structure. Each of these new compounds were then examined at 77° as well as at room temperature. Some of these compounds were  $\text{Fe}^{++}$  and  $\text{Fe}^{+++}$  complexes. Special precautions had to be taken for the  $\text{Fe}^{++}$  complexes, since these were in the reduced state. All synthesis had to be carried out in a dry box and the sample sealed prior to taking the spectroscopic absorption measurements. Table V lists the names and results of all the porphyrin compounds (set A) that were examined.

The main conclusion from our studies, already reported on earlier, is that data for molecular absorptions in liquids differ greatly from those in solid matrix suspensions. Whereas the porphyrin spectra looked sufficiently suggestive to continue the experimental search using a large number of porphyrin compounds (see Tables III and V) and under a variety of conditions, the hydrocarbon data did not even remotely suggest the slightest similarity to the diffuse interstellar spectra. Furthermore, all the porphyrins studied in this survey showed anomalous behavior for the Soret band under solid matrix suspension techniques.

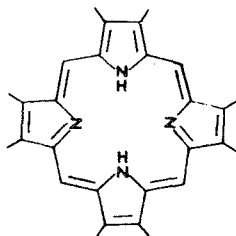
The following conclusions can be drawn from the solid matrix suspension data of porphyrins, low temperature studies of all the hydrocarbons, and the composite absorption mixtures (Fig. 14): although qualitative features are suggestive of interstellar lines for the porphyrin compounds, the variations that can be introduced by the technique employed as well as the nonreproducibility and the lack of



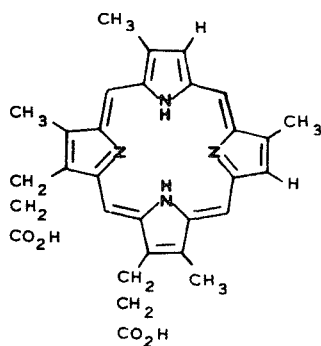
sharpness of the lines particularly the virtual absence of a strong Soret absorption line, eliminates both the technique as well as the samples (Set A of Table 3) for interstellar absorption candidates. The diffuse interstellar lines do not therefore originate in solid grains, neither do they arise from impurities in grains. Since the carbonaceous chondrites however do show the presence of various types of hydrocarbons, this general survey studies undertaken here might prove of interest in that work. These studies do not rule out the existence of molecules of Tables IV and V entirely, however they do preclude their discovery in the optical region of the spectrum with the sensitivity presently available to astronomers.

\*  
TABLE V  
EXPERIMENTAL RESULTS  
LIQUID NITROGEN SPECTRA OF PORPHYRINS (TECHNIQUE A)

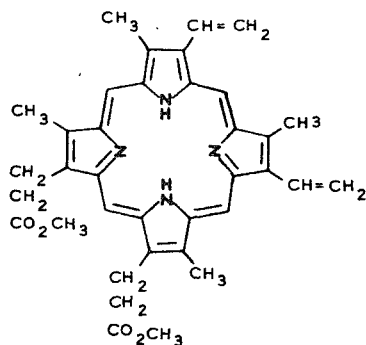
General Formula:



Name _____	Formula _____	$\lambda_{\text{max}}$ (Soret) _____	Comment _____
---------------	------------------	--	------------------



Deuterioporphyrin IX  
dimethylester



Protoporphyrin IX  
dimethylester

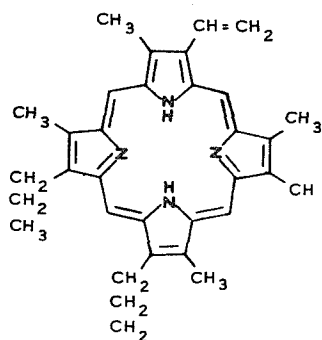
\* Dr. C. E. Castro kindly assisted in the construction of Table V.

Name

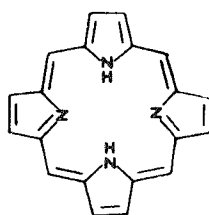
Formula

$\lambda_{\max}$   
(Soret)

Comment



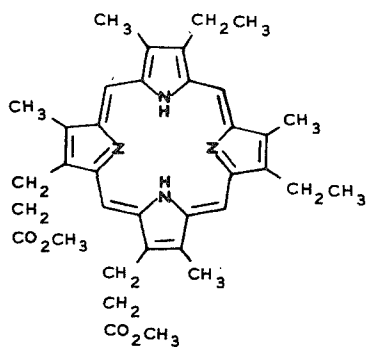
Protoporphyrin IX



4045 (S)  
3900 (S)

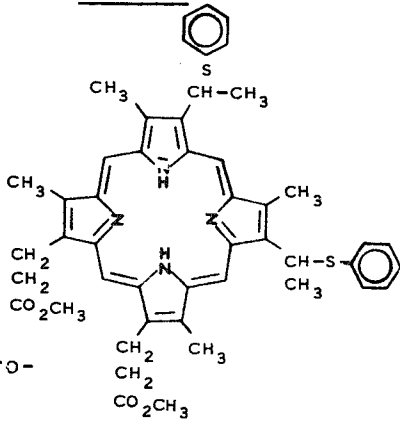
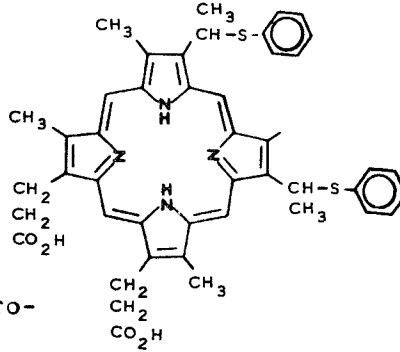
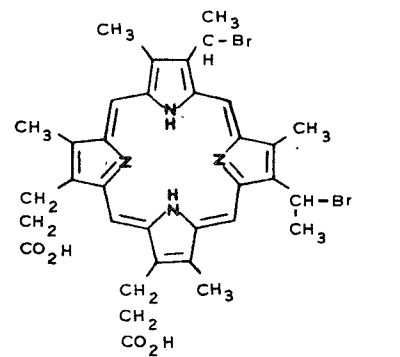
Room Temp.  
" "

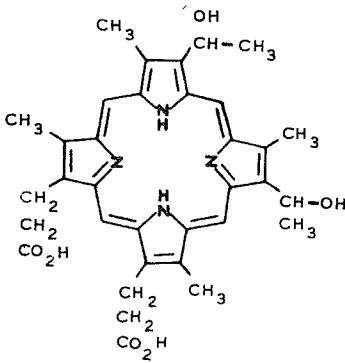
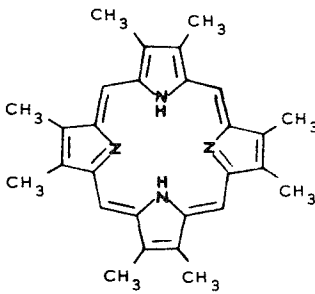
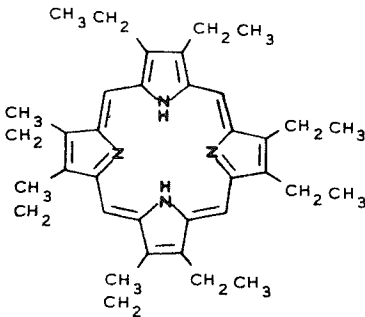
Porphine



3925 (M)  
3970

Mesoporphyrin IX  
dimethylester

Name	Formula	$\lambda_{\max}$ (Soret)	Comment
2,4-di- $\alpha$ -thio-phenylethyldeutero-porphyrin IX dimethylester		4400 (B) 4040 (M-S) in $\text{CHCl}_3$ 4050 (B) 4050 (B)	EPA glass Room Temp. Grease & glass powder Grease & $\text{Al}_2\text{O}_3$
2,4-di- $\alpha$ -thio-phenylethyldeutero-porphyrin IX		4000 (B) "	EPA glass EPA Room Temp.
2,4-di- $\alpha$ -bromo-ethyldeutero-porphyrin IX		4150 (B)	

Name	Formula	$\lambda_{\text{max}}$ (Soret)	Comment
Hematoporphyrin		4000 (M) in $\text{CHCl}_3$	Room Temp.
Octamethyl- porphyrin		3855 (B)	
Octaethyl- porphyrin		3975 (B) 4075 (B)	

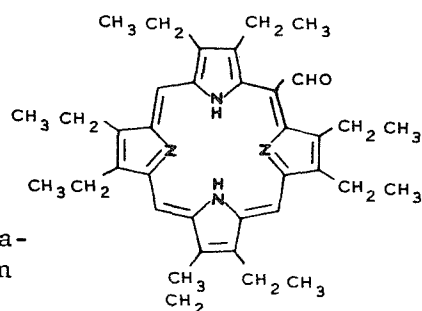
Name

Formula

$\lambda_{\max}$   
(Soret)

Comment

Mesoformylocta-  
ethylporphyrin

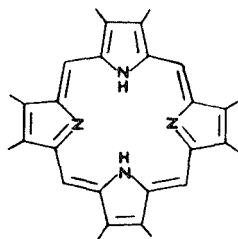


3960 (B)

# PORPHYRINS

General formula:

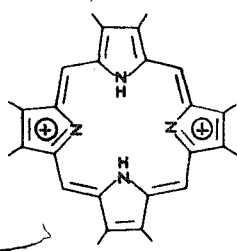
See previous pages  
for specific  
skeletons



<u>Porphyrin</u>	<u><math>\lambda_{\text{max}}</math></u>	<u>Comment</u>
Mesoporphyrin IX dimethylester	3925 (M) 3970	Diff. Conditions
Protoporphyrin IX dimethylester		
2,4-di- $\alpha$ -thiophenylethyl- deuteroporphyrindimethylester	4400 (B) 4040 (M-S)	EPA Glass $\text{CHCl}_3$ Room Temp.
2,4-di- $\alpha$ -thiophenyldeuteroporphyrin	4000 (B)	EPA Glass
Hematoporphyrin	4000 (M)	in $\text{CHCl}_3$ Room Temp.
Octamethylporphyrin	3855 (B)	
Octaethylporphyrin	3975 (B) 4075 (B)	
Meso-Formyloctaethylporphyrin	3960 (B)	
Porphine	4045 (S) 3900 (S)	Room Temp.

# PORPHYRIN DICATIONS ( $\text{CF}_3\text{CO}_2\text{H}$ )

General formula:



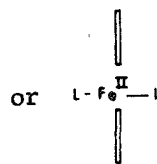
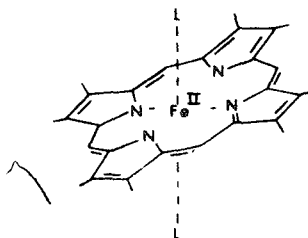
See porphyrin list for substituent variations.

<u>Porphyrin Dication ( Porp <math>\text{H}_2^{\text{H}}</math> )</u>	<u><math>\lambda_{\text{max}}</math></u>	<u>Comment</u>
Mesoporphyrin IX dimethylester $\text{H}_2^{\text{H}}$	4030 ( M )	
Protoporphyrin IX dimethylester $\text{H}_2^{\text{H}}$	4050 (VB)	
2,4-di- $\alpha$ -thiophenylethyldeutero- porphyrin dimethylester $\text{H}_2^{\text{H}}$	4100 (B)	
2,4-di- $\alpha$ -thiophenylethyldeutero- porphyrin $\text{H}_2^{\text{H}}$	4050 (B)	
Hematoporphyrin $\text{H}_2^{\text{H}}$	4045 (B)	
Octamethylporphyrin $\text{H}_2^{\text{H}}$	4000 (B)	
Octaethylporphyrin $\text{H}_2^{\text{H}}$	4025	
Meso-Formyloctaethylporphyrin $\text{H}_2^{\text{H}}$	4235 (M) 4520 (M)	



# IRON (II) COMPLEXES

General formula



end on

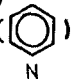
L = ammonia ( $\text{NH}_3$ )  
or pyridine<sup>3</sup> (pyr. i.e., )

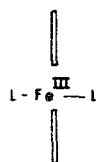
Porphyrin skeleton	$\text{Fe}^{\text{II}}$ Porp ( $\text{NH}_3$ ) <sub>2</sub>	$\text{Fe}^{\text{II}}$ Porp ( )
Mesoporphyrindimethylester	3930 (M)	4055 (M), 4445
Protoporphyrindimethylester	3980 (M)	4295 (B)
Octaethylporphyrin	3945 ( M)	3950 (M)
Deuteroporphyrin IX	4125 (B)	4020 (M)

# IRON (III) COMPLEXES

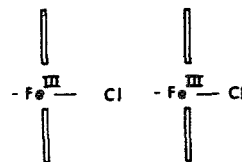
General formula:

(end on)

L = ammonia (NH<sub>3</sub>)  
or pyridine ()

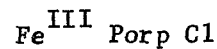
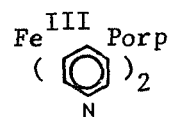
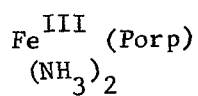


also



for hemin

Porphyrin skeleton



Mesoporphyrindimethylester

3935

3950 (M)

Protoporphyrindimethylester

3970 (M)

4040 (B)

3975  
3940 (Rm.Temp.)

Octaethylporphyrin

3905 (M)

Deuteroporphyrin

3910

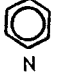
4000 (B)

3975 (M)

# MISCELLANEOUS PORPHYRIN SPECIES

<u>Compound</u>	<u><math>\lambda_{\max}</math></u>	
Cytochrome C ( $\text{Fe}^{\text{II}}$ )	4145 (VS)	
Cytochrome C ( $\text{Fe}^{\text{III}}$ )	4105 (S)	
Chlorophyll A	4430, 4440 (M) 4375	Room Temp.
Chlorophyll B	4550 (S) 4650 4380	Room Temp.
(Note: all of the above are isolated molecules i.e., the protein prevents porphyrin-porphyrin interactions.)		

## COPPER COMPLEX

		OctaE ( $\text{Cu}^{\text{II}}$ ) (  ) <sub>2</sub>
Octaethylporphyrin ( $\text{Cu}^{\text{II}}$ )	4410 (M)	4370

SECTION 3  
RESULTS--CONTINUED

3.1 THE TETRABENZPORPHINES, TECHNIQUE B

First, a survey of these and related compounds was undertaken (see Table VI) using a variety of techniques and conditions. From this data we concentrated on Mg TBP dipyrindine. It was instructive to examine the spectra of molecule  $\chi$  under a variety of conditions. The first series of experiments involved room temperature measurements at different concentrations. Fig. 15 shows a series of such runs using the solvent pyridine. Note that at the lowest concentration, A, only the Soret band at  $4420\text{\AA}$  is recognizable. As the concentration is increased other features become recognizable. (A and B of Fig. 15 are actually at the same concentration, however the path length was increased from 3mm for A to 10mm for B).<sup>\*</sup> Curve D is for a path length of 10 cm. E is pyridine alone in a 10 cm long cell. F is for another solvent, namely, T.E.A. Figure 16 shows the results of a series of runs using T.E.A. as solvent. Note the shift of the Soret band to shorter wavelengths ( $4300\text{\AA}$ ). The same concentration but a 3mm and 1 cm cell respectively, are represented by curves A and C of Fig. 16, taken at room temperature. Curve B of Fig. 16 is for a solution of Mg TBP + 2CN in EPA at  $77^{\circ}\text{K}$  producing a transparent "glass" matrix. Some additional structure in the spectra is apparent. The background slope indicates some cluster-type association, resulting in scattering.

Following these studies, we concentrated exclusively on Mg TBP + dipyrindine (molecule  $\chi$ ). The technique B, which has successfully demonstrated the presence of  $\chi$  molecules involved suspension of these molecules in an inert matrix using "isolation" Shpols'kii techniques.

<sup>\*</sup>(A) 3mm cell, 10:1 dilution; (B) 1cm cell, 10:1 dilution; (C) 3mm cell, original strength; (D) 10cm cell, 100:1 dilution.

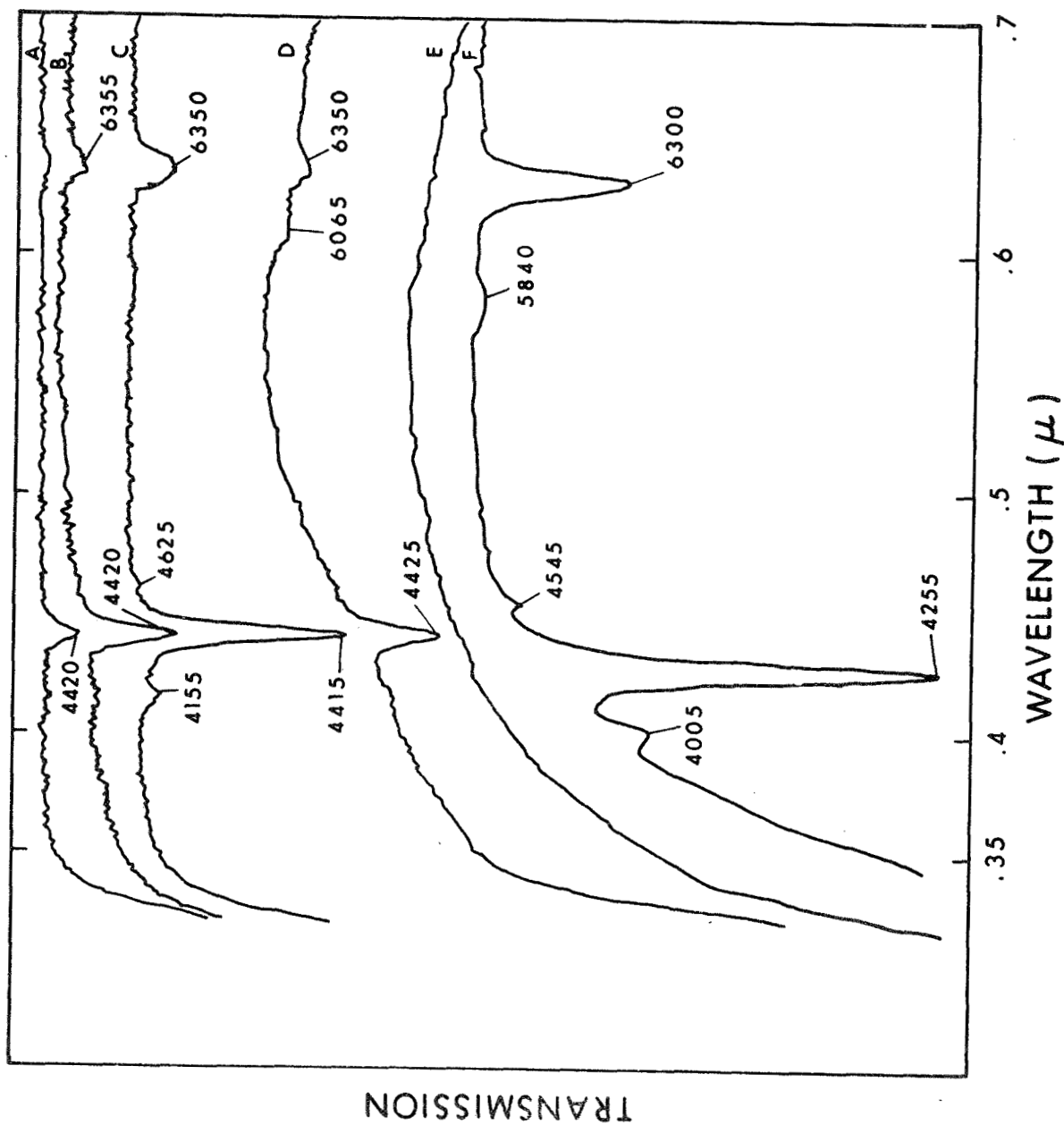


Figure 15. Molecule X: Typical Room Temperature Data (see text)

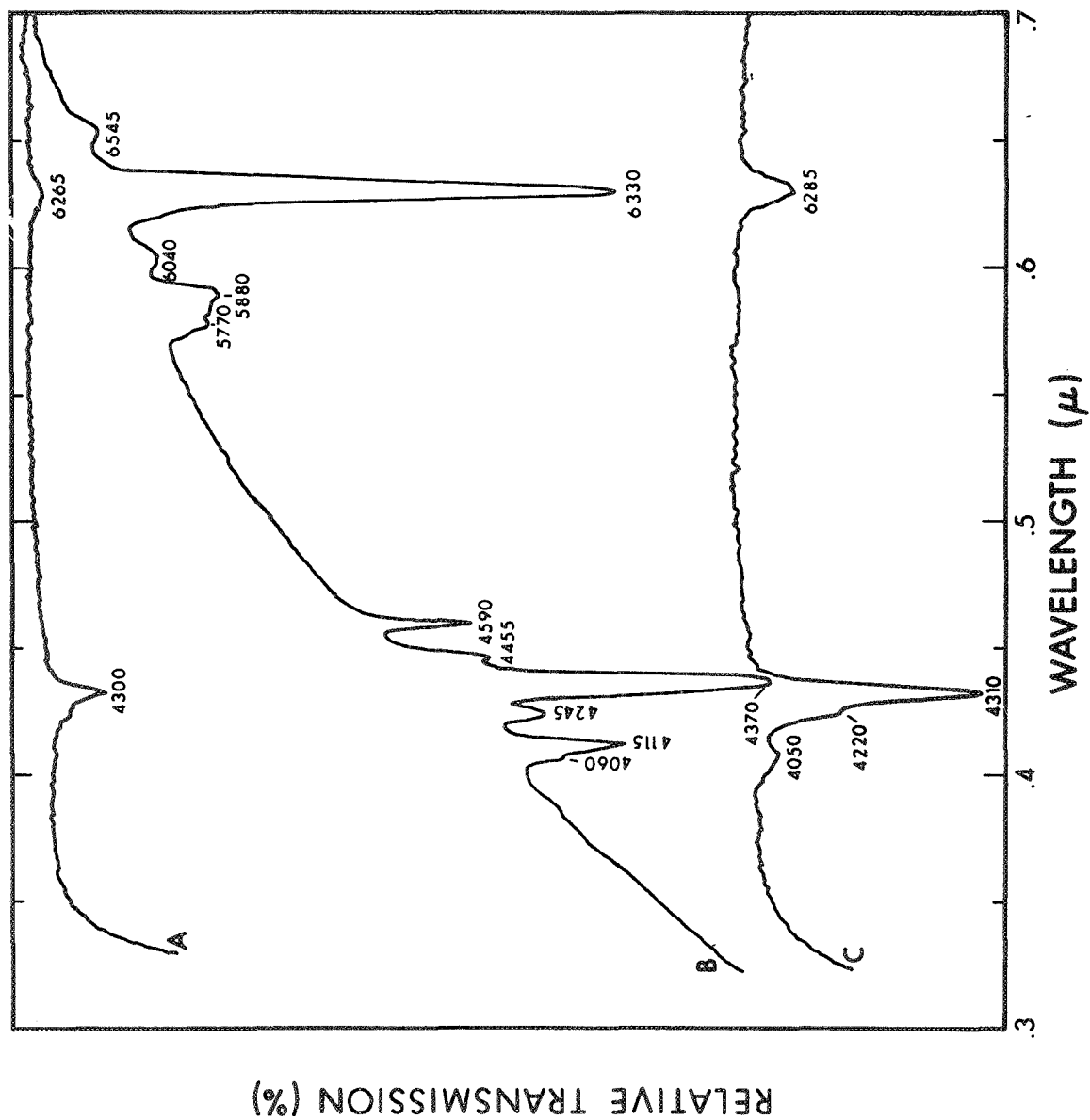


Figure 16. A - MgTBP in EPA (3 mm cell)  
 B - MgTBP + 2CN in EPA liquid glass at 77°K  
 C - MgTBP in EPA Room Temperature (1 cm cell)

TABLE VI

## TBP &amp; Pc SURVEY DATA

(All data Precision  $\pm 10\text{\AA}$ )

	CONDITION	SOLVENT	TEMP.	"4430"Å	"6284"Å	
Zn TBP	Vapor	*	>500°C	Absent	6275	Broad Line
	Vapor	*	>500°C	Absent	6240	" "
	Vapor	*	>500°C	Absent	6290	" "
(1) Mg TBP	Vapor	*	>500°C	Absent	6350	4700 (250Å wide) 5400 (130Å wide) 5460 med. 5925 weak 5875 weak 5860
(2) Mg TBP	Liq.Dewar	N.Octane	Room	4250	6305	4350w, 4700w, 4800w, 5030w,
(3)	Liq.Dewar		Room	4252	6295	5080, 5130, 8 small lines 5200-5600
(4)	Solid Dewar	N.Octane	Liq.N <sub>2</sub>	4430	6270	4300 fine structure & emission lines at 6600Å doublet
(5)	Solid Dewar	N.Octane	Liq.N <sub>2</sub>	Vanished	6275	6345
(6)	Diluted Solid			Vanished	Vanished	6345 fine structure & emission lines at 6600Å doublet
(7)	Dilute	N.Octane		Vanished	Vanished	4270 4350 4455 weak, 5950, 6000, doublet 6040 strong, 6070, 6080, 6120, 6130, sharp emission: 6580, 6600 doublet
(8)	Liquid	Pyridine	Room	4430 4430	6360 6345	

TBP & Pc SURVEY DATA  
(Continued)

	CONDITION	SOLVENT	TEMP.	"4430"Å	"6284"Å	
(9)	Solid Concentrated	Pyridine	Liq.N <sub>2</sub>	4430	6280	4615, 4170, 5260, 5800, 5900, 6050
(10)	Dilute	Pyridine	Liq.N <sub>2</sub>	4430		
	Concentrated			4430	6290	4170
MgPc	Liquid 10mm cell	Pyridine	Room			6150 sharp, 3445, 6820, 1.956μ
FePc	Liquid	Pyridine	Room			6000, 6630, 3280
Castro #14 2 axial pyridine						
Mg TBP	Liquid	Pyridine	Room	4410	6355	6550, 4155, 5435, 4605 weak Weak Broad
Mg TBP	Vac.deposited on quartz		Room	4450 (broad 250Å wide) at 1/2 max.		6550 (250Å wide)
Zn TBP		N-Octane	Room	4275 (80Å wide)	6300 (100Å wide)	4040 weak, 4555, 5320, 6035 weak
Zn TBP		decane	Room	4275	6260 6270	4145, 4420, 4550, 6490
Mg TBP		Chloron. Si grease	Room Room	4360 4600 wide	6424 6500	4105, 4660, 5940, 3450 6000 all wide

\* 1" Quartz Cell.



TBP & Pc SURVEY DATA  
(Continued)

Zn TBP	EPA	Room Temp.	3975	4215	4425	4520	5950	6220	6450
Zn TBP	EPA	Room Temp.	4020	4250	4300	4370	4560	5955	6220 6450
Doublet									
Mg TBP	Pyridine	LN <sub>2</sub>	4165	4420	4620	5925	6375		
Mg TBP	Pyridine	LN <sub>2</sub>	4160	4425	4630	5910	6340		
			4175	4430	4640	5905	6360		
TBP	T.F. Acid	Room Temp.		4250			6670		
broad									
Mg TBP	1:1 EPA- Triethylamine TEA	LN <sub>2</sub>	4150	4270	4475, 4610 sharp	5915	6320		
Zn TBP	1:1 EPA-TEA	Room Temp. LN <sub>2</sub>	3990 4100 4230	4245 4350	4600, 4465 sharp	5780	sharp 6285		
Mg TBP	EPA	Room Temp.	4055	4310			6285		
EPA	LN <sub>2</sub>		4100 4200	4350	4575	5800 shallow	6255		
Mg TBP	EPA + KCN	Liq. N <sub>2</sub> Glass	4060 4245	4370	4455 4590	5770 5880 6040	6330 sharp		
Mg TBP	5:1 EPA:TEA	Liq. N <sub>2</sub>	4145 4260	4395 (4465) w	4600 sharp	5775 5900	6305		

TBP & Pc SURVEY DATA  
(Continued)

Mg TBP	KBR Pellet	Room Temp.	4350 saturated	6000	6350 6465 (No IR abs. to 3μ)
		Liq. N <sub>2</sub>	~4360	5900	6350
Zn TBP	Chlorona pth	Room Temp.	4110 4380	5879	6370
Mg Pc	Chlorona pth	Room Temp. 3450		6155	6820 7048
Fe Pc (#14)	Pyridine				6550 Broader & More intense
Fe TPB	Pyridine	Room Temp.	4310 sharp		6000 broad
Mg TBP	Silicone grease	LN <sub>2</sub>	4050 (150A)	5800	6350, 6765

This enables the molecules to be separated from each other since we showed from our previous studies that it was the presence of adjacent molecules that caused the undesirable broadening of the Soret band, for instance. Figure 17 shows the Soret absorption band of molecule  $\chi$  at 77°K, its line width at half power points is 40Å, moreover, the peak of the absorption coincided within experimental error with the astronomically observed line at 4428Å. A large number of additional spectroscopic coincidences were observed. These results are described in Table VII. The set of coincidence wavelengths which are bracketed in Table VII do not have the same weight (due to the lower S/N) as the other data.

Other weaker transitions were also observed. These provide good candidates for checks of the model, provided more sensitivity is attainable with the astronomical observations. Note that 16 coincidences were established of the laboratory 77°K data and the diffuse interstellar lines.

As will become apparent in the subsequent discussions, the physical conditions under which molecule  $\chi$  exists in outer space is somewhat different from our laboratory condition. Hence, the precise matching of 16 lines with the indicated precision speaks well for the "isolation" technique employed.

The only experimental difficulty was the blending of about 3 lines in the 6284Å region in absorption. This difficulty was partially overcome by fluorescence techniques.

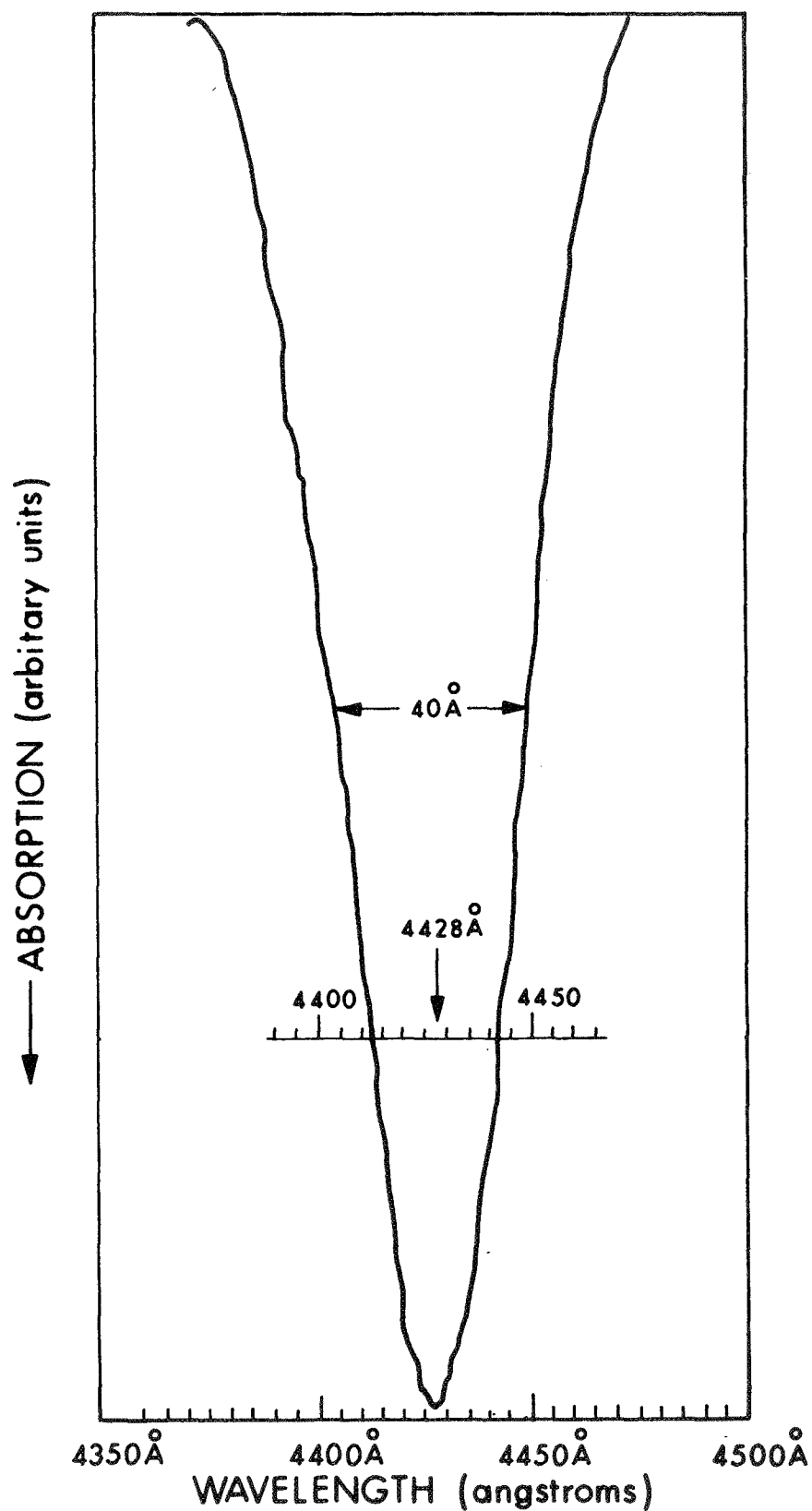


Figure 17. Laboratory Measurement Soret Band of Molecule X

TABLE VII  
LABORATORY MEASUREMENTS ON MOLECULE  $\chi$   
AT 77°K

<u>LABORATORY MEASUREMENTS</u>			<u>REMARKS</u>	<u>ASTRONOMICAL DATA</u> ***	
<u>No. of Independent Observations &amp; Measurements</u>	<u>Mean Wavelength <math>\text{\AA}</math> (<math>\pm 2\text{\AA}</math>)</u>	<u>Width <math>\text{\AA}</math></u>		<u>Absorption</u>	<u>Width</u>
6	4428	40	Soret (0, 0) State A	4428	20
1	4883**	14		4883	40
1	(4761) <sub>w</sub>	2		4762	4
2	5422	6		5420	10
1	(5448)	2		5448	14
2	5486 <sub>5</sub>	3.5		5487	5
2	5704	3		5705	4
2	5776	10		5778	17
2	5781	2		5780	2.5
2	5798 <sub>5</sub>	1.5		5797	1.2
1	(5843) <sub>w</sub>	2		5844	4
2	5849	1.5		5850	1
2	6174	10	(0, 0) State B	6175	30
1	(6175)	25	" "		
1	6284	<2	Emission line†	6284	4
1	6614	<2	Emission line†	6614	1
1	6663	<2	Emission line†	6661	1

\* The  $\lambda 6284$  absorption region consists of an unresolvable blend of 3 possible lines. Fluorescence gave sharp line.

\*\* 4883 $\text{\AA}$ : superimposed on this weak band seems to be a Triplet at  $\lambda\lambda 4877$ , 4883, 4890.

\*\*\* This data was kindly supplied by Dr. G. H. Herbig for H.D. 183143. We are greatly indebted to him for providing this critical data prior to publication.

† Observed by fluorescence techniques.

### 3.2 IR SPECTRA

In view of the success in matching the diffused interstellar lines with laboratory spectra in the optical regime, it is reasonable to inquire whether other spectral regions offer possible additional corroborative evidence. There is a paucity of laboratory UV data on  $\chi$ . The astronomical data by Stecher gives essentially a single strong broad absorption band centered at  $2100\text{\AA}$  (plus some other possible structure).

Very strong UV absorptions are predicted for many hydrocarbons e.g. benzene and pyridine, but the astronomical data is not available. The situation is better in the IR. See Table IX for a list of astronomical absorption lines taken from the recent literature. Since each absorption line is weak, it was expedient and necessary to take the average of all the data. The wavelength precision is about 2% for the astronomical data and 1/2% for laboratory data. Table X also lists the major IR absorption lines of molecule  $\chi$  corresponding to the IR astronomical data. Table VIII shows our measurements of four porphyrin IR spectra taken on two different spectroscopic laboratory instruments\*. The samples were prepared by incorporating  $\chi$  powder material in KBr pellets. It is noteworthy that the strongest IR absorption lines of molecule  $\chi$  are accounted for by the interstellar spectra, with the exception of the line at  $693\text{cm}^{-1}$  which falls outside the region of accessible interstellar IR absorption data, due to atmospheric absorption.

Since our IR data on molecule  $\chi$  is consistent with six of the IR astronomical absorption lines and allowing for the poor quality of these preliminary and very difficult astronomical measurements, we feel our interpretation presents a stronger case than the published

---

\*Perkin Elmer, Block Engineering (Digilab). We are indebted to Dr. Peter R. Griffiths of Block Eng. Co. for kindly taking a duplicate set of measurements on the Digilab instrument, whose sensitivity and resolution was greater than that of the Perkin Elmer instrument. The values quoted in Table VIII are averages from both sets of data.

interpretation which matches only two lines using (Mg, Fe) Si O<sub>3</sub> and olivine as the suggested absorbing molecules. Moreover, olivine presumably does not match any of the diffuse interstellar lines whereas molecule  $\chi$  does. (Also, three additional astronomical lines at 950 and 775 as well as 1135cm<sup>-1</sup> can be matched with the strongest IR absorption lines in TBP (or porphin), bringing the total of IR lines to nine for possible assignment to porphyrin molecules.) This needs further analysis.

---

R. F. Knacke et. al., Ap. J. 155, p. 189 (1969)

TABLE VIII

IR ABSORPTION MEASUREMENTS (cm<sup>-1</sup>)

<u>(<math>\chi</math>)</u> <u>MgTBP</u>	<u>H<sub>2</sub>P<sub>c</sub></u>	<u>Porphin</u>	<u>FeTBP</u>
			2985
1590m		3300w	2930
1475w	1485m	1530w	
1465m			
1455m			
1430m	1420m	1410m	
1400m			
1322m	1320s		
1287m	1305s		
	1285s		
1232s doublet	1260s		1260
	1170m	1222m	1245
1212m	1140m	1135m	1220
1110vs	1100vs		1100
1115s	1080s		1070
			1060
1051 triplet		1050m	
1032			
1014			1010
1000m	990vs	970vs	
887m	860vs	950vs	
		900w	
823s		850vs	
		840vs	
753vs	730vs	770vs	755
737vs	718vs	740w	735
	712vs	725s.	700
703	700s	715s	
693* s.v. sharp	665w	690vs	
620w	600m		
610w doublet	475w		
	415m		

w = weak, m = medium and s = strong

\* 693 =  $(231 \pm 1) \times 3 \text{ cm}^{-1}$



TABLE IX

## IR ASTRONOMICAL ABSORPTION SPECTRA

Object	Interstellar IR Absorption Lines (Microns)					
1. R. Aquarii	7.8s	8.8w	9.7w	11.2	12.7	12.7
2. 119 Tauri	7.8w or 8.0	8.8	9.7s	10.6		
3. $\alpha$ Boo	7.8	9.1		11.2	12	12.8
$\alpha$ Her	7.8	9.7		11.0	12.1	12.9
$\alpha$ Ori	7.8	8.8			12.2	13.5
$\mu$ Cep	(7-9) wide feature with structure			11.0w	12.2	
	8.5					
$\chi$ Cyg	7.8	9.1		11.0		12.9
O Cet	(7-9) wide				12.2	13.3
4. NML Cygnus Circum- stellar		9.2w				13.5

## References:

1. W. Stein et.al. Ap. J. (Letters) 155, L3 (1969).
2. R. F. Knacke et.al Ap. J. 155, L187 (1969) (Suggested orthopyroxene).
3. F. C. Gillett et.al. Ap. J. 154, 677 (1968)(Suggest circumstellar matter).
4. W. Stein et.al. Ap. J. 155, L177 (1969).

TABLE X

---

 INTERSTELLAR IR LINES AND LABORATORY SPECTRA
 

---

Summary of IR

Astronomical Data:

<u>Mean Spectra</u> ( $\mu$ )	7.8	8.8	9.1	9.7	(10.6)	11.1	12.2	12.8	13.5
<u>Astronomical</u> ( $\text{cm}^{-1}$ )	1280	1140	1100	1030	(950)	900	820	780	740

F. M. Johnson

Lab Spectra of  
 Molecule  $\chi(\text{cm}^{-1})$ 

	1287m, 1232s-1110s	1051 triplet	1000, 887	823s	-	753vs	737vs
TBP	1160	(935, 968w)		830	780w		732, 718v
H <sub>2</sub> P <sub>c</sub>	1285s	1140 1100vs	1080s				
Porphin	1135	1050m	950vs	850vs	770vs		725s
	C-H Vibn in plane	C-H Vibn. in plane		C-H out of plane			N-H

---

TABLE XI

Porphin Bands	Interpretation of IR Spectra
1110, 1144 $\text{cm}^{-1}$	Ring breathing vibration of pyrrole. (Opposite rings undergo out-of-phase vibration, for symmetry $E_u$ in $D_{4h}$ ).
770 $\text{cm}^{-1}$	In-phase combination (symmetry $A_{2u}$ in $D_{4h}$ ) or an out-of-plane pyrrole ring deformation vibration which absorbs 838 $\text{cm}^{-1}$ in pyrrole itself.
830-880	Out-of-plane C-H groups.
1048, 1184, 1224	In-plane deformation modes of C-H.
3036, 3102, 3181	Allowed stretching modes of C-H.
<hr/>	
<u>Cu Pc Bands</u>	
735-775	C-H out of plane vibration.
1000-1300	C-H in plane hydrogen bonding.
1470-1510	C-C ring stretching.
1600-1700	C = N stretching bands.

### 3.3 THERMODYNAMIC TESTS ON MOLECULE $\chi$

Two types of test were performed on powder material of  $\chi$  in order to ascertain its chemical stability. The first involved sealing a few milligrams of  $\chi$  in a 1 inch quartz vial under high vacuum. This vial was heated to 500-600°C while optical transmission measurements were performed. The characteristic green color was observed due to the strong molecular absorption band in the 6350Å region. Spectroscopic measurements were made during the entire heating cycle. The same experiment was repeated without vacuum sealing the quartz vial, i.e. in air, and obtaining substantially the same results.

A more critical test on  $\chi$  verified that the molecules do not get destroyed on heating to 500°C, but merely sublime. The equipment for these measurements involved a molecular beam oven filled with a few milligrams of  $\chi$ . The oven had a small orifice which permitted the  $\chi$  molecules to escape (when the oven was heated >500°C) and settle on a quartz plate some 6 inches from the beam orifice (see Fig. 18). A green deposit was obtained on the plate, which was examined spectroscopically and found to contain molecule  $\chi$  in its original constitution (see Table VI for data).

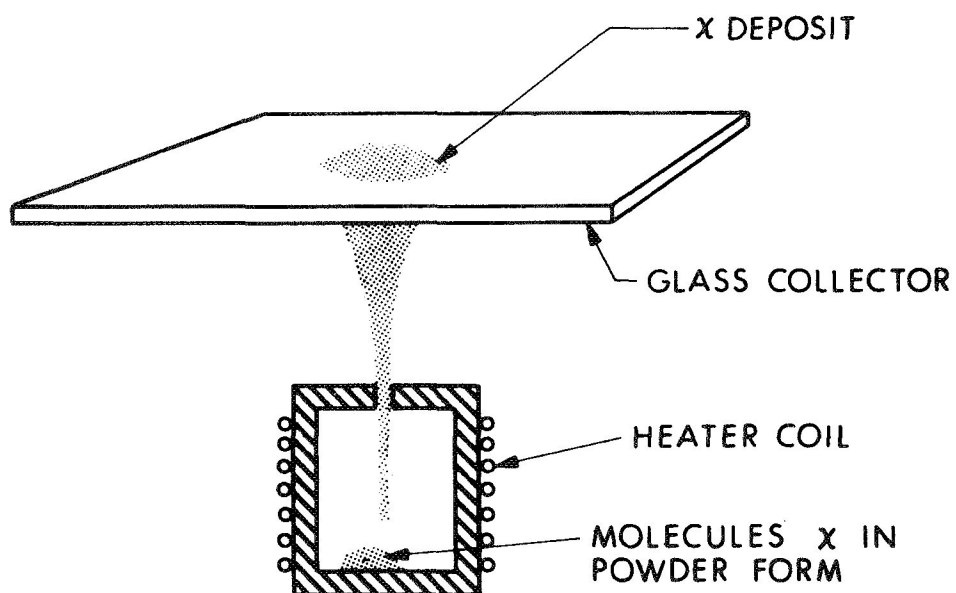


Figure 18. Molecular Beam Apparatus Equipment to Demonstrate Sublimation of  $\chi$  Molecules at  $\sim 500^{\circ}\text{C}$

### 3.4 FLUORESCENCE DATA

Fluorescence room temperature data of the major tetrabenzporphin (TBP), Pthalocyanines (Pc) and tetraphenylporphin (TPP) compounds was taken by means of the Aminco phosphorimeter. The room temperature data are collected in Table XII. Such data are of importance in the theoretical interpretation of the spectra leading ultimately to more precise assignments of energy levels and transition assignments of these related compounds. The data are not of high precision, and hence will only be used for qualitative comparison studies. More precise fluorescence data were obtained of MgTBP and FeTBP at 77°K using the sensitive high precision scanning equipment. The low temperature data are, therefore, far more valuable in the theoretical interpretation. They showed some lines both in absorption and in fluorescence yielding the (0,0) assignments. Moreover, the  $\lambda_{6284}$  line had a much narrower line width in emission than the corresponding absorption blend of about three lines, referred to previously.

### 3.5 COMPLEXING OF PORPHYRIN MOLECULES

We performed a large number of experiments on changing the appendages of the basic porphyrin molecule. Of course, the basic porphin macrocycle molecule allows an almost infinite variety of appendages or side chains to be attached to the eight corner positions as well as the four methene bridge-carbon atoms. The enormous variety of molecules are discussed by Falk.\* We investigated a significant variety of such molecules, as shown in this report. The bulk of these porphyrins are

---

\*J. E. Falk, "Porphyrins and Metalloporphyrins", Elsevier Publ. Co. (1964).

TABLE XII

FLUORESCENCE DATA  
Molecules Dissolved in Solvent - Room Temperature (Amino)

COMPOUND	EMISSION SET AT $\lambda$	EXCITATION $\lambda$				EXCITATION SET AT $\lambda$	EMISSION
Mg TBP in octane	6400	3320w	4280s	6100m	6300m		
Mg TBP conc. in octane	6400	3350w	4280s	6195s	6300s	4030 shoulder	4420s 6400m
TBP (sublimed)	6500	3400 broad, w	3900	4090	4220s	4380s	
					5280vw	5640m	
					6090bw	6620	
TBP	4880	3400	3945	4210w	4430w	4640s	4880 5010 6530- 6720 broad emiss.
		b, st.	shoulder				
Mg TPP in pyridine	6280	3480	3800	4480	5300w	5700s	3950w 6380 broad b, st 4650 6380 broad
		broad		sharp st	6510w		
MgPc in pyridine	7000	None	None	None	None	None	None None
H <sub>2</sub> P in pyridine	6700	3370w					
	3370	3500			6800w		
Mg TBP in pyridine dense sample	6460	4100	4215	(4430 ABS)	5880	6220	6460 sharp sharp
					sharp		
Mg TBP	6500	4130s	4310s	4430s	5900m	6380s	
1-Chlorona- phthalene		sharp	sharp	sharp			
Zn TBP	6400		4300s				
1-Chlorona- phthalene				5810w	6310s		4430 6400

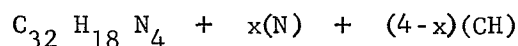
# FLUORESCENCE DATA

Molecules Dissolved in Solvent - Room Temperature (Aminco)

COMPOUND	EMISSION SET AT Å	EXCITATION Å	EXCITATION SET AT Å	EMISSION
Fe TBP pyridine	4800	3320 4080 (~ 4200 4640 abs)	4080 4800 3220 4790b	
Mg TBP pyridine	6500 4900	3250w 4100w (4430 5470vw 5880s 6240s 6420s broad abs) shallow sharp sharp 4230w abs.	3250 3645w 3940 4310w 4100 4500w 4205 4660s 4600 5880 6240	4960s 6400w broad broad 4930 6400w 4920s 6430m b 4905s 6460s b broad 4910 6540m b 6250- 6500 st broad 6460 b st



found in nature.\* Another variety of porphyrins, however, can only be obtained by either laboratory (or astro) synthesis. These are the porphyrins with four benzene rings attached at the end of each pyrrole unit. Another synthetic but less stable variety has the four benzene rings attached to the methene bridge-carbon atoms.\*\* There are however, as has been pointed out previously, only two very important varieties because of their thermodynamic stabilities: the Pthalocyanines and the Tetrabenzporphins, where in the former the methene bridge atom is nitrogen and in the latter it is carbon. Hybrids of the two are possible, thus:



for x = 0	Tetrabenzporphin
x = 1	Tetrabenzmonazaporphin
x = 2	Tetrabenzdiazaporphin
x = 3	Tetrabenztriazaporphin
x = 4	Pthalocyanine

In addition, there is a large choice for central atom, e.g., H<sub>2</sub>, Mg, Fe, Zn, etc. These compounds were synthesized and extensively studied by Linstead and his group as part of a long series of studies.

Returning now to our original studies, we noted that it is relatively easy to remove the central atom or to attach molecular groups on the central atom. Note that when the central heavy atom is removed, it is replaced by two hydrogen atoms. Since the 4428<sup>0</sup>Å interstellar line however can only be simulated in the laboratory with Mg as the central atom and two pyridine groups attached to the central atom, it was important to study the effects of substituting other groups to the central atom. These experiments were performed at room temperature.

---

\*Table V lists representative porphyrins found in nature, which we examined.

\*\*TPP.

using the inert solvent octane. As can be seen from the data in Fig. 19, each of the groups,  $C_5H_5NH_2O$ ,  $H_2CO$ ,<sup>\*</sup>  $NH_3C_5H_5N$  caused a shift of the Soret band indicating that indeed these groups attached themselves to the Mg atom. We performed one low temperature experiment with the  $NH_3$  radical attached to the Mg atom and found that at low temperatures ( $77^\circ K$ ), the Soret band is shifted to  $4340\text{\AA}$ , whereas it is  $4428\text{\AA}$  using pyridine. This is a significant result since some of the additive groups have recently been identified in the interstellar medium by radioastronomy.<sup>\*\*</sup> There is one molecule however, which attaches itself readily to the pyridine molecule that is water, (in fact pyridine and water are completely miscible). This fact led to a series of experiments which are described next in the section on reddening.

### 3.6 REDDENING

Since Trumpler's discovery of color excess in 1930, a great deal of astronomical investigation has centered on the study of the wavelength dependence of extinction<sup>\*\*\*</sup> (called reddening). A rough  $1/\lambda$  dependence was generally recognized. Through the work of Nandy, Underhill and Walker and others this wavelength dependence of the interstellar "dust" can in fact be well represented by two straight lines which meet at about  $4430\text{\AA}$ . Whereas J. M. Greenberg in his analysis chose to disregard this change in slope, G. Herbig<sup>\*\*\*\*</sup> makes a strong point of its potential significance. Before we discuss our results, which bear directly

---

\*

\*\* The ammonia and water molecules in the interstellar medium were discovered by investigators under the leadership of C. H. Townes.

\*\*\* Good general references and surveys to the field are found in H.L.Johnson "Interstellar Extinction", Chap. 5, in "Nebulae and Interstellar Matter" ed. by B.M.Middlehurst & L.H.Allen. J.M.Greenberg "Interstellar Grains", Chap. 6 of same volume.

\*\*\*\* G. H. Herbig, I.A.U. Symposium No. 31, (1967).

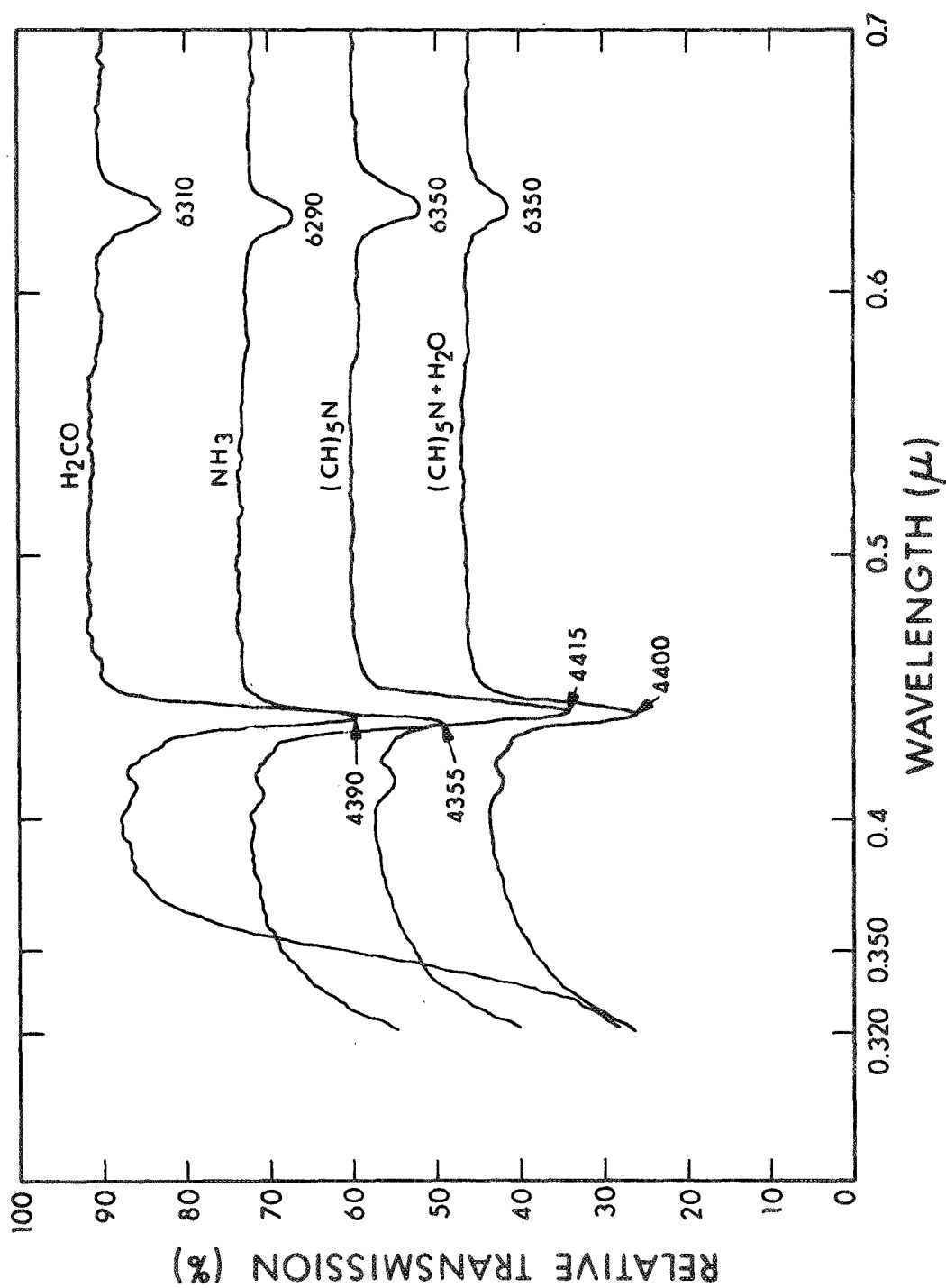


Figure 19. Molecular "Add-Ons" to MgTBP

on this astronomical observation, let us briefly review the general interrelationship of dust, reddening and diffuse lines. (1) There is a fairly good relationship between reddening and the strength of the diffuse interstellar lines. Also the strength of all interstellar lines generally go together.\* (2) The reddening is not well correlated with the strength of interstellar atomic lines, mainly because they are saturated. Hence most astronomers have generally considered that the carrier responsible for the diffuse lines is somehow associated with the "dust" grain. The following hypotheses were considered:

- (1) Carrier imbedded in grain
- (2) Carrier on surface of grain
- (3) Grain and carrier separate (this would not give a good reddening and diffuse line correlation)

There lies the general dilemma: if the carrier were inside the grain, then the diffuse absorption line should have a strong asymmetric shape as theoretically evaluated by J. M. Greenberg and proven in our early experimental studies, (see e.g., Figs. 6 and 7). Since the careful astronomical measurements by G. H. Herbig\*\* show a perfectly symmetric line shape for 4430, one has to rule out hypothesis (1). Furthermore, as was pointed out in our Final Report No. 1 (1967) p. 65, possible arbitrary matrix shifts could cause shifts and eventual broad smear of interstellar lines by as much as  $100\text{\AA}$ ; another impossible situation. Some astronomers suggest very small grains, as Van de Hulst requires. However, Greenberg\*\*\* shows theoretically an asymmetric  $\lambda 4430$  line shape for even very small grain sizes if impurity atoms are imbedded in the grain. Even if the carrier molecule were sitting on some

---

\* G. H. Herbig, I.A.U. Symposium No. 31, (1967).

\*\* G. H. Herbig, Z f. Astroph. 64, 512 (1966).

\*\*\* J. M. Greenberg, p. 356 of his survey paper, loc cit.

hypothetical grain surface, electric field perturbations are sufficient to alter the free atom spectra. This too was proven experimentally, using small glass beads as "grains".

Now here is the horn of the dilemma: if one postulates that the "reddening" particles and the carriers of the diffuse lines are one and the same particles, then a molecule, even a big one like a porphyrin, is of insufficient size to bring about the desired Mie scattering (reddening) and reproduce the astronomical  $1/\lambda$  scattering curves.

The solution to the dilemma is aggregation of the identified interstellar molecule X into clusters of roughly the size of  $(1/10)\lambda$ . One simple method of complexing X molecules into a loosely bound structure is via molecules of  $H_2O$  which can easily attach themselves to the 2 pyridine molecules of each X molecule. Mr. M. Dubin<sup>\*</sup> has suggested that the recently discovered water complexes<sup>\*\*</sup> might have a bearing on our problem. In order to investigate experimentally the X molecule complexing phenomena, we dissolved X molecules in an inert liquid matrix (octane) at room temperature. A small amount of water was added and the solution briefly vibrated. A cloudy appearance of the solution indicated that the desired complexing was being accomplished. Spectroscopic studies were undertaken on the three different solutions in 1 cm cuvettes, and the results are shown in Fig. 20. The top curve A is obtained with X molecules dissolved in octane with no water nor complexing taking place, resulting in complete absence of reddening. The lower curves B and C show two different solutions with different degrees of complexing. The strength of the Soret absorption band gives a measure of the amount of X molecules present, (molar extinction  $\sim 6 \times 10^5$ ) whereas the slope of the "reddening" curve gives a measure of the amount of aggregation assuming one has an independent measure on the cluster size distributions. The latter quantity was not obtained in these preliminary investigations. However, the most notable phenomena to be observed in curves B and C are the

---

\* M. Dubin, private communication.

\*\* L. C. Allen & P. A. Kollman, Science 167, 1443 (1970).

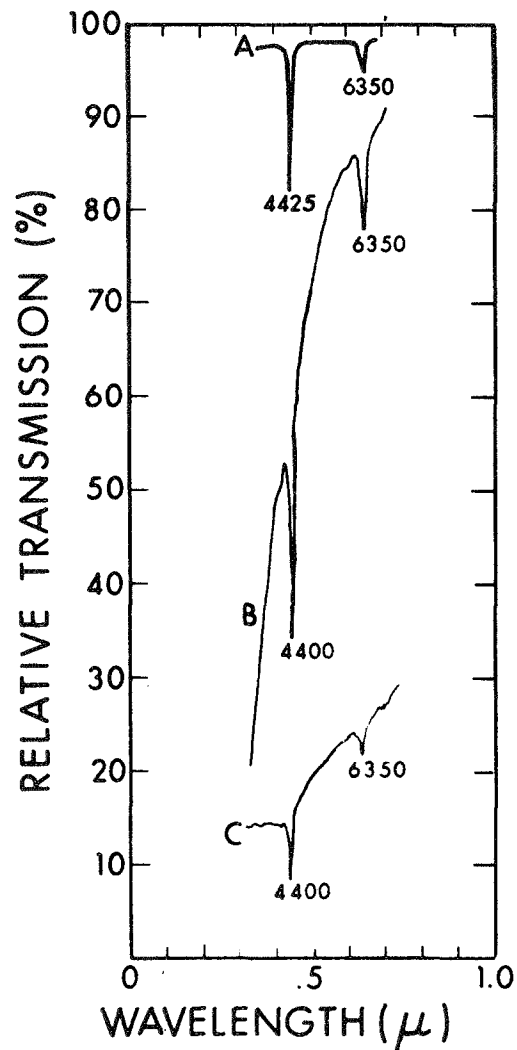


Figure 20. Aggregation of  $\chi$  Molecules to Simulate Reddening:

A - No aggregation

B - Various degrees of  $\chi$  association

C - Various degrees of  $\chi$  association

(Note break in slope on short wavelength side of 4430 in curve C)

clearly recognizable changes in slope on the short wavelength side of  $\lambda 4430$ . This effect corresponds to the astronomical case and suggests very strongly the conclusion that part of interstellar reddening in certain regions of the galaxy is due to clusters of X molecules. If this hypothesis proves correct, then X molecules in interstellar space can be simply identified by the change in slope at  $\lambda 4430$ .

The review paper by H. L. Johnson (loc. cit.) gives examples of a variety of extinction curves and a variety of associated critical wavelengths for slope changes, suggesting the presence of unidentified molecular complexes other than X in the interstellar medium. The change in slope of the reddening curve following an electronic transition (such as the Soret band at  $\lambda 4430$ ) can be understood from the work of Van de Hulst.\* Using his notation, the extinction efficiency factor is:

$$Q_{\text{ext}} = x^4 \operatorname{Re} \frac{8}{3} \frac{\frac{m^2}{2} - 1}{m^2 + 2}^2 + \dots - \operatorname{Im} 4x \frac{\frac{m^2}{2} - 1}{m^2 + 2} + \dots \quad (1)$$

where  $x = ka = 2\pi a/\lambda$                        $a =$  particle radius

$m = n_1 - in_2 =$  complex refractive index

$C_{\text{ext}} = \pi a^2 Q_{\text{ext}} =$  Total extinction cross-section

Now from standard treatments of dispersion,\*\* the refractive index can be related to the molecular polarizability,  $\alpha$ , which in turn can be shown to be related to the fundamental properties of the molecule including

---

\* H. C. Van de Hulst, "Light Scattering by Small Particles", John Wiley & Son, (1957) p 191, 270.

\*\* See e.g., M. Born & E. Wolf, "Principles of Optics", MacMillan Co., pp 90-95 (1959), C. Kittel.

frequency and its resonant frequency  $\omega_{ij}$ , as follows:

$$\frac{n_1^2 - 1}{n_1^2 + 2} = \frac{4\pi}{3} \sum N_i \alpha_i \quad (2)$$

$$\alpha = \frac{e^2}{m} \sum \frac{f_{ij}}{\omega_{ij}^2 - \omega^2 - i\omega g} \quad (3)$$

$$f_{ij} = 2\omega_{ij} m |X_{ij}|^2 / \hbar \quad (4)$$

where,  $f_{ij}$  = oscillator strength  
 $X_{ij}$  = matrix element for transition  $j \rightarrow i$   
 $e, m$  = charge and mass of electron respectively  
 $g$  = damping term  
 $\hbar$  = Planck's constant/ $2\pi$

It is well known and can be easily seen from the above quotations (3) that the polarizability changes on resonance  $\omega = \omega_{ij}$ . This is called "anomalous dispersion". Furthermore, the polarizability  $\alpha$ , has a different value for  $\omega > \omega_{ij}$  than for  $\omega < \omega_{ij}$ . Now since  $\alpha$  is directly related to the refractive index, from equations (2) and (3), it is easily seen how the left hand side of equation (2) would assume different values depending on whether  $\omega < \omega_{ij}$  or  $\omega > \omega_{ij}$ , which in turn directly relates to the extinction cross section (equation (1)). Hence if  $\omega_{ij}$  corresponds to  $\lambda 4430$ , whose electronic transition probability is large ( $f \sim 1$ ), then the change in slope on either side of  $\lambda 4430$  is qualitatively explicable.

Precision measurements of this effect should be performed in the next phase of the follow-on program.



As a rough check on our hypothesis, consider the following: it is well known from the study of dielectrics that the dielectric constant  $\epsilon (=n_1^2)$  changes abruptly as a function of wavelength following an electronic transition. Now the dominant factor in equation (1) is the factor

$$q = \frac{n_1^2 - 1}{n_1^2 + 2},$$

where the real part  $n_1$ , of the complex index of refraction  $m$  is taken. Let us examine a few typical values of this factor ( $q$ ):

	n	1	1.25	1.5	2.0	2.5	3.0
$\frac{n^2 - 1}{n^2 + 2} = q$		0	0.156	0.295	0.5	0.637	0.73

It is readily seen that a small change in the value of  $n$ , particularly for values of  $n$  close to unity, a very marked change in the factor  $q$  is produced, which in turn will change the scattering function, as seen from equation (1).

### 3.7 DISCUSSION ON THE ORIGIN OF X

It might be worth while to ponder on the possible origin of the interstellar molecule X which is widely dispersed throughout the galaxy and the more closely packed hydrocarbons and occasional porphyrins found in carbonaceous chondrites. We believe that the X molecules originate very early in the evolution of a "solar" system presumably in association with the comets whose highly elliptic and high velocity orbits would enable these molecules, loosely bound to cometary nuclei, to be carried far into outer space. The carbonaceous chondrites presumably were formed later, perhaps at the time of the asteroid belt, in the development

of the solar system. Thus, the presence of carbonaceous material and occasional presence of porphyrins might be due to somewhat different conditions such as higher density, higher temperatures and temperature gradients, tighter packing, as loosely formed chondrules coalesce via weak gravitation forces.

The cometary material is presumably primarily composed of hydrocarbons of the  $\chi$  molecule variety or other similar compounds in a very loose structure, such that when it encounters the sun on successive return trips, the outer material easily becomes vaporized and ionized and hence exhibits the spectroscopic lines that are associated with such disintegration products as CH, CN,  $\text{CH}^+$ ,  $\text{C}_3$ , and  $\text{C}_2$ .

Although porphyrin astrosynthesis is briefly discussed in Scientific Report No. 1, some additional comments will be made here. The following questions may be asked: "Are atomic interstellar abundances adequate? Why is Mg and not Fe the central atom? How come Tetra-benzporphine and not Pthalocyanines are formed?" Indeed,  $\chi$  molecules are composed of the most abundant elements, H, C, N, and Mg. The reason why Mg rather than Fe is favored must relate to the early development stage of the protosolar nebular out of which the components for the cometary objects were formed. The reason for TBP rather than Pc synthesis is directly related to the stellar abundance ratio of  $\text{CH}/\text{CN} \sim 10$  to 25. Namely for TBP the ratio  $\text{CH}/\text{CN}$  is 5 and for Pc,  $\text{CH}/\text{CN} = 2$ . Consequently, the production of TBP is strongly favored over Pc by a factor of between (25 - 60) to 1. Since there could be further unidentified lines in the interstellar spectrum, it is not unlikely that TBP, monoazo, diazo or triazo compounds are potential candidates and should be examined in the follow-on program, i.e., (1) removal of central atom and successive substitution of C atoms at the methene bridge position by N atoms. When all four methene bridge carbon atoms of TBP have been replaced by nitrogen, one obtains pthalocyanine (Pc).

### 3.8 INTERSTELLAR MICROWAVE EMISSION FROM H<sub>2</sub>O

The discoveries<sup>\*</sup> of microwave emission from H<sub>2</sub>O and absorption for NH<sub>3</sub> raised a particular interesting question for H<sub>2</sub>O, since its 6<sub>15</sub>-5<sub>23</sub> emission arises from a state 446 cm<sup>-1</sup> above the ground state. Since there have been reports<sup>\*\*</sup> of association of IR stars with H<sub>2</sub>O emission, and the fact that some of these stars have IR absorption spectra consistent with that of molecule  $\chi$  (See Section 3 ) as well as our data on H<sub>2</sub>O- $\chi$  clusters, opens up the question whether H<sub>2</sub>O molecules in association with  $\chi$  could be excited to the 6<sub>15</sub> state by energy transfer from the parent molecule or whether H<sub>2</sub>O and  $\chi$  molecules receive the IR radiation from the same source. If the  $\chi$ -H<sub>2</sub>O complex is pertinent, then a great number of questions can be asked: Would the H<sub>2</sub>O- $\chi$  complex allow or hinder the rotationally observed 6<sub>15</sub>-5<sub>23</sub> transitions? Is the space density of  $\chi$  molecules sufficient? Our estimate of 10<sup>11</sup>-10<sup>12</sup>  $\chi$  molecules in a 1 cm<sup>2</sup> square column is low compared to the estimates of 10<sup>16</sup> to 10<sup>18</sup> per cm<sup>2</sup> for H<sub>2</sub>O.

There is no question that clusters of  $\chi$  molecules make excellent light traps, however many details would still have to be investigated if a correlation between the H<sub>2</sub>O microwave emission at 22.2 GHz, and the possible energy transfer mechanisms (such as radiationless transitions for  $\chi$  molecular excited states to the H<sub>2</sub>O molecule are both possible and allowed, or indeed necessary (since both molecules could independently receive IR pump radiation from a common source)).

---

<sup>\*</sup>A. C. Cheung, D. M. Rank, C. H. Townes, D. D. Thornton, W. J. Welch, Nature, 221, 626 (1969); Phys. Rev. Lett., 21, 1701 (1968).

<sup>\*\*</sup>P. R. Schwartz and A. H. Barrett, Ap. J., 159, L123 (1970).

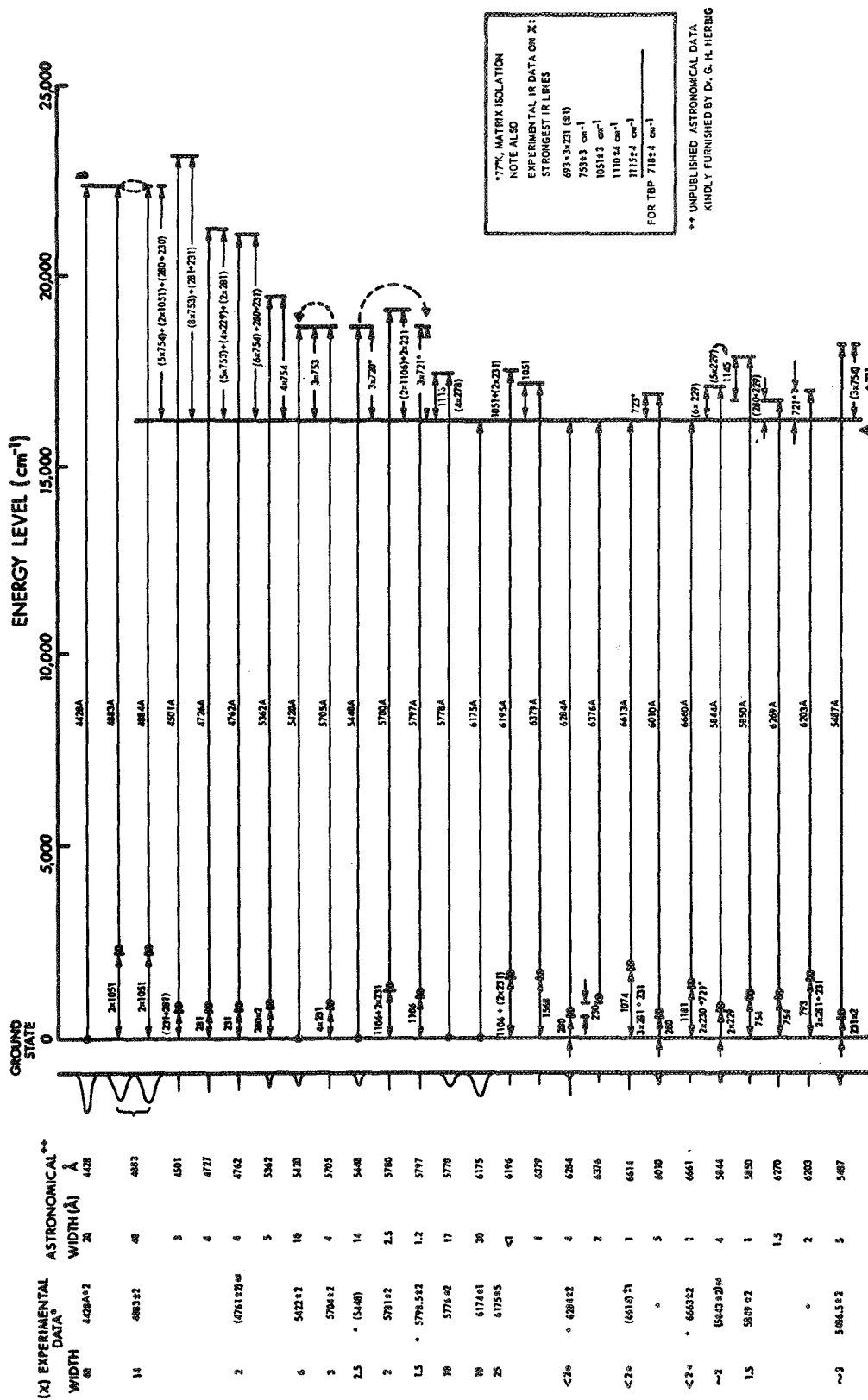
### 3.9 ANALYSIS OF DATA

As a first approximation to the construction of an energy level diagram for the X molecule, the astronomical observations of the diffuse interstellar lines for a particular star\* (H.D. 183143) were arranged so as to conform to the observed IR data and consistent with the laboratory observations of two distinct electronic states in the visible region, at  $\lambda 4428$  and  $\lambda 6175$ , marked A and B respectively. A fair degree of internal self-consistency was obtained; however, no claim is made for uniqueness. (See Fig.21.) The most striking result from such a preliminary arrangement of vibronic states is the fact that a fraction of the interstellar lines originate from states which are not in the ground state. Since our measurements on molecule X were taken as 77°K, the absence in our lab spectra of certain astronomically observed lines becomes explicable. In fact, all astronomically observed transitions from the ground state have been observed in the laboratory spectra. The laboratory observed lines in fluorescence at  $\lambda\lambda 6175$ , 6284, and 6613\*\* all originate from the lowest vibrational level of the electronic state A. Other vibronic states predicted from this model give rise to weaker laboratory observed transitions in the 4000 to 4500Å region. (These would be observable astronomically were it not for blending of stellar hydrogen lines.) One can predict to a precision of 1Å a hitherto unobserved diffuse interstellar line:  $5205 \pm 1\text{Å}$ , E.W. = 0.2, width  $12 \pm 2\text{Å}$ .

It should, in principle, now be possible to construct potential curves and examine each transition on the basis of the Franck-Condon principle. From such an energy level diagram and astronomical data giving absorption line intensities, it should also in principle be possible to compute an effective vibrational temperature, provided thermodynamic equilibrium exists in the region of these molecules. It is clear from

---

\*This data was kindly contributed by Dr. G. H. Herbig.



this analysis that the interstellar molecules must be at some temperature considerably higher than the conventionally accepted 20°K. An attempt to invoke the sum rule by plotting the function\* Y vs G seemed puzzling at first.

$$Y = \log \sum_v \frac{I_{abs}^{v'v''}}{\nu} = C - \frac{G''(v'')hc}{kT}$$

where  $G''(v'')$  is the vibrational state energy ( $\text{cm}^{-1}$ )

$I_{abs}$  is line absorption intensity (E.W. in Å)

T is the effective temperature

C is a constant

h, e, k have their usual meanings

However, by separating the "starred" transitions, i.e., those involving the  $721 \text{ cm}^{-1}$  vibronic excitation, distinct "temperatures" were obtained. The " $\chi'$  or  $721 \text{ cm}^{-1}$  molecule", presumably a trivial off-shoot from molecule  $\chi$  (perhaps TBP)<sup>\*\*</sup> has an effective temperature of  $1000^\circ\text{K}$  (Fig. 22) whereas the  $\chi$  molecules are in an extremely hot radiation environment. In fact, from the slope of Fig. 23 it is  $-2200^\circ\text{K}$ , i.e., population inversion, via optical pumping has taken place. The  $6284\text{\AA}$  transition seems to belong to the "starred" molecule (indicated by squares in Fig. 22). The  $4883\text{\AA}$  point corresponding to  $2 \times 1051 \text{ cm}^{-1}$  is unambiguous and consequently the data points cannot be connected in any way other than a negative slope, with the implication of population inversion, due to radiative pumping. (The only possible ambiguity in level assignments arises for states having equal vibrational components in both ground and excited states. This ambiguity was resolved on the basis of line width and intensity.) Thus, by arranging the astronomical lines according to a scheme which is self-consistent and accounts for the strongest vibronic IR transitions, one arrives at the astounding conclusion that, (1) IR maser action associated

\* G. Herzberg, "Molecular Spectra", I, van Nostrand (1950), p. 204.

\*\* or  $\chi$  complex--dimer, trimer, etc. Since  $\chi$  and  $\chi'$  share the electronic state A, their relationship has to be close.

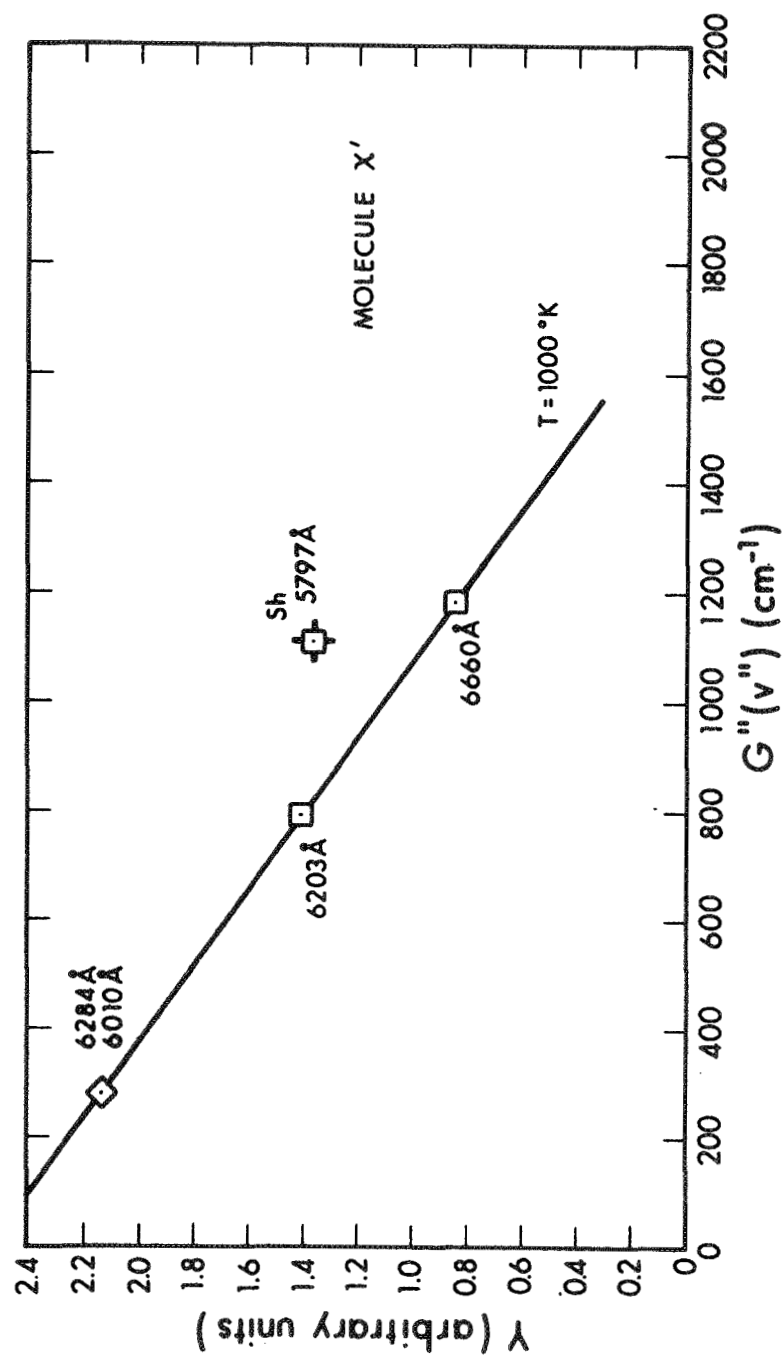


Figure 22. "Boltzmann" Plot for  $\chi'$  (presumably an aggregate of  $\chi$ )

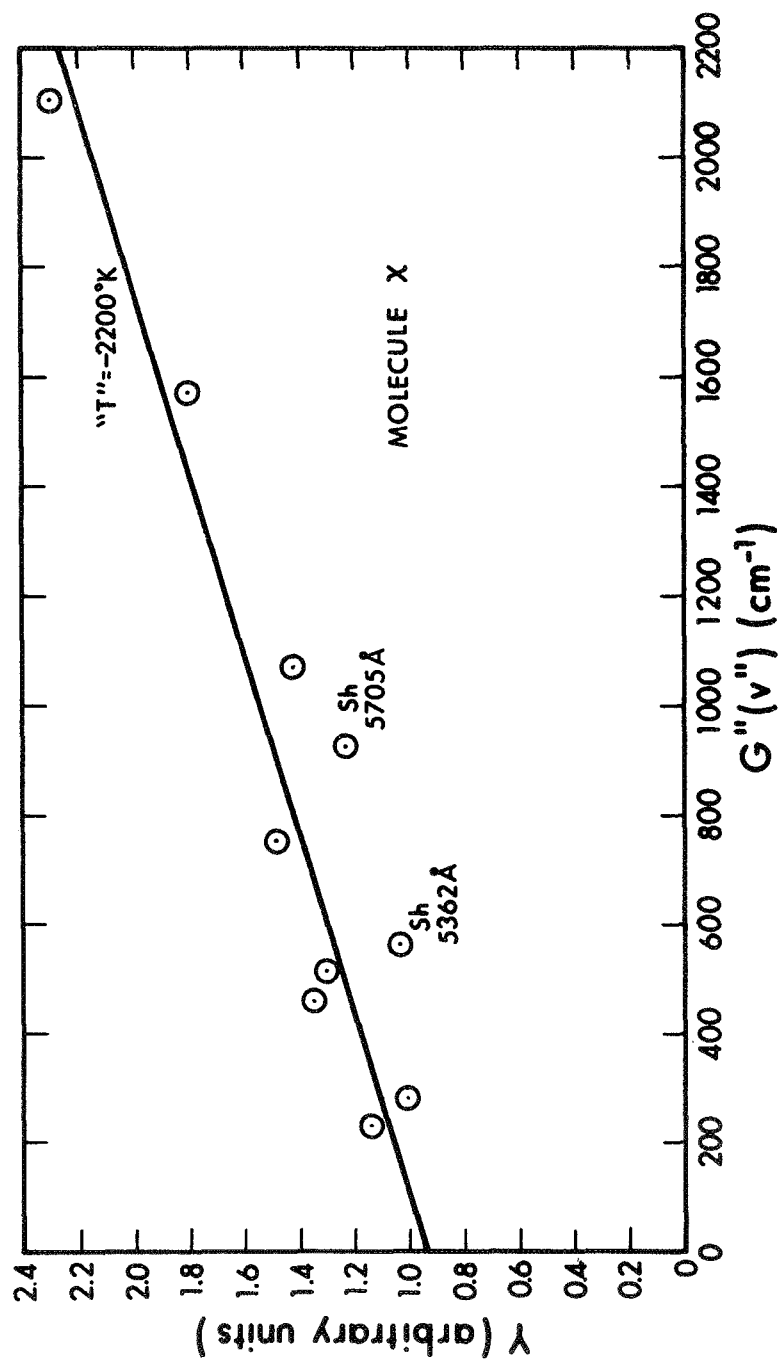


Figure 23. "Boltzmann" Plot for X



with  $\chi$  molecules is possible and presumably in progress, (2) indeed, non thermal equilibrium obtains, (3) all the relatively sharp interstellar diffuse lines (line widths of about  $1\text{\AA}$ ) are associated with vibronic excited states, which on the basis of our analysis, are excellent candidates for maser emission. Conversely, the IR maser action presumably accounts for line narrowing of those diffuse interstellar transitions whose line widths are of the order of  $1\text{-}2\text{\AA}$  instead of  $10\text{-}30\text{\AA}$ .

The following prediction<sup>\*</sup> can therefore be made: Intense IR emission line sources should exist at 754, 1106, 1051, 1074, 1181, 1568, 2102  $\text{cm}^{-1}$ , as well as other related wavelengths in association with stars having strong diffuse interstellar lines.

### 3.10 LINE WIDTH

The diffuse astronomical lines have widths that vary from  $1\text{\AA}$  to  $40\text{\AA}$ . If we postulate that the molecule  $\chi$  can exist either by itself or in clusters, then the minimum observed line width might be due to the range of accessible rotational lines.

The moment of inertia (I) of molecule  $\chi$  about an axis perpendicular to its basal plane is roughly  $3.2 \times 10^{-36}$  c.g.s. Now

$$B = \frac{h^2}{8\pi^2 c I}$$

---

\*

As a historical footnote and digression, it might be of interest to point out that the author discussed maser action in the interstellar medium, particularly population inversion associated with nebulae, in 1963 at the American Physical Society Meeting in Pasadena, Calif., --at least 2-3 years before interstellar maser action was discovered. Maser action in grains was first suggested by the author in 1954 at an Astronomy Department seminar at Columbia University, in connection with possible sources for nonthermal galactic radiation components.

so that

$$B = 8.6 \times 10^{-4} \text{ cm}^{-1}$$

It is now possible to compute the range of J values for different assumed temperatures, using the expression\*

$$J_{\max} = 0.5896 \sqrt{\frac{T}{B}} - 1/2$$

$T_{\text{OK}}$	$J_{\max}$
20	90
500	450
1000	635
2000	900

If the minimum line width is due to unresolved rotational structure, then its width would be roughly  $4BJ$  or more precisely

$$\Delta\nu_{\text{PR}} = 2.3 \sqrt{BT},$$

where the difference between the peaks of the P and R branches is given by  $\Delta\nu_{\text{PR}}$ . Using  $T = 2000^{\circ}\text{K}$ , one obtains  $\Delta\nu \approx 3 \text{ cm}^{-1}$ . Thus,  $\Delta\lambda \sim 1\text{-}2\text{\AA}$  which corresponds to about the minimum observed diffuse interstellar line width. Presumably, the wider lines are due in part to molecule-molecule interactions. The transitions arising from the ground state invariably are broader than those arising from the excited vibronic states. The lab data for  $\chi$  molecules frozen in a matrix prevents rotational motion. Moreover, the  $4428\text{\AA}$  width was found to be concentration dependent. It is of interest to compare our predictions of maser action in the  $\chi$  molecules with recent astronomical observations of microwave emission from  $\text{H}_2\text{O}$  molecules associated with a transition which lies  $446 \text{ cm}^{-1}$  above the

---

\* Herzberg, loc. cit. p. 124.

ground state. Thus confirming the possibility of an optical pumping mechanism (IR radiation) which possibly applies to both  $\text{H}_2\text{O}$  and  $\chi$  molecules.

The 4883 $\text{\AA}$  line: The 4883 $\text{\AA}$  diffuse interstellar line has the broadest width, namely 40 $\text{\AA}$ , of all the observed lines.<sup>\*</sup> Its explanation is presumably connected with the observation that its upper state can be one of two states lying at the level B (22583  $\text{cm}^{-1}$  above the ground state). Hence, we shall postulate that the potential curves associated with the two electronic states intersect, giving rise to overlapping of the eigenfunctions.<sup>\*\*</sup> Thus, upon absorption of the 4883 $\text{\AA}$  photon into the upper state B, its energy can very efficiently be transferred to an upper vibrational state associated with the electronic state A, giving rise to "coriolis interaction",<sup>\*\*\*</sup> and thus accounting for its unusually broad line width. (See Fig. 21.)

The experimental difficulty of taking these measurements needs to be reemphasized:

- A. At high temperatures (500 $^{\circ}\text{C}$ ) with the molecules in a closed container in the gas phase, the frequent molecular collisions cause a far too rapid molecule-molecule type interaction. (In the

---

<sup>\*</sup> Using the data for H.D. 183143 kindly supplied by G. H. Herbig.

<sup>\*\*</sup> See Herzberg loc. cit. p. 286, (Vol. I).

<sup>\*\*\*</sup> G. Herzberg, Vol. III, p. 118.

interstellar medium, the collision mean free path is undoubtedly far greater, however the interstellar molecules are very likely in the proximity of an intense radiation field.)

- B.
1. In a frozen matrix at 77°K some degrees of freedom are removed.
  2. At low laboratory concentrations, the dominant lines only are observed. Allows precision 4428Å measurement.
  3. At high concentrations, at 77°K, in a matrix, additional weak spectral lines are observed. 4428Å however becomes exceedingly broad at these high concentrations.
  4. At very high concentrations, the Fe and the Mg complex of TBP form molecular aggregates which give rise to a new weak set of lines at 77°K in the red region of the spectrum. These transitions are still being analysed. Their lines were studied in emission and absorption. If such complexes exist in the interstellar medium, then these spectra are of interest in the interpretation.
  5. Preliminary results of low temperature Fe TBP aggregates:
    - a. New (0, 0) band at  $\lambda\lambda 6581$   
6595
    - b. Removal of degeneracy causing splitting of lines
    - c. The 6581 and 6595 were obtained in both emission and absorption
    - d. Energy difference between pairs of lines, gave the following vibrational energy differences 279, 783, 1059, 1112, 1298, and 1594 cm<sup>-1</sup> for FeTBP
    - e. The Mg TBP aggregate gave an identical (0, 0) band at  $\lambda\lambda 6581$  and 6595Å. However the other weak emission lines were different from the Fe TBP spectra.

### 3.11 SUMMARY OF ENERGY LEVEL DIAGRAM

It is worthwhile to reexamine the energy level assignments for internal consistency (see Fig.21). Note that only the strongest of the allowed (and observed) IR transitions in molecule  $\chi$  are utilized. The strongest and sharpest observed IR transitions and the number of times they are invoked per state in constructing the energy level diagram for both ground and excited states are shown in the table:

<u>Vibronic Energy (<math>\text{cm}^{-1}</math>)</u>	<u>No. of Times</u>
231*	21
280	13
1051	5
1106	4
754	10
721	5
1113	1

(A variation of  $1 \text{ cm}^{-1}$  in the vibrational transition is ignored for the purpose of this compilation.)

These vibronic energy states are characteristic of molecule  $\chi$  and add strong confirmation to the 16 laboratory spectral lines which coincide with the astronomical data. The exception is the vibrational energy of  $721 \text{ cm}^{-1}$  which presumably is associated with TBP or some other simple derivation of molecule  $\chi$ . The lower vibrational energy of  $721 \text{ cm}^{-1}$  compared to  $754 \text{ cm}^{-1}$  is similar to changes seen in  $\text{H}_2\text{Pc}$  and Porphin, where the central metal atom is replaced by 2 hydrogen atoms.

\*One of the strongest and sharpest lab IR transitions in molecule  $\chi$  is at  $693 = 3 \times (231 + 1) \text{ cm}^{-1}$ , indicating the presence of  $231 \text{ cm}^{-1}$ . (Our laboratory equipment did not extend to that long wavelength region of  $231 \text{ cm}^{-1}$ , hence the indirect  $231 \text{ cm}^{-1}$  line.)

### 3.12 INTERSTELLAR ABUNDANCES OF MOLECULE $\chi$

Based on the observed mean equivalent width of  $3\text{\AA}$  kparsec in the  $\chi_{4428}$  band,<sup>\*</sup> it is possible to estimate the space density of  $\chi$  molecules. If we take the value of  $nf$  computed by Dressler,<sup>\*</sup> where  $n$  is the number of absorbers and  $f$  is the oscillator strength, then  $nf = 6 \times 10^9 \text{ cm}^{-3}$ . Since  $f \cong 1$ , and the molecular weight of  $\chi$  is 690  $n = 6 \times 10^{-30} \text{ gm/cm}^3$ . Now, according to Purcell,<sup>\*\*</sup> the interstellar grain density in space must exceed  $2.5 \times 10^{-27} \text{ gm/cm}^3$ , consequently no more than 0.2% by weight of interstellar "dust" is responsible for the diffuse interstellar lines (and some of the reddening).

It is also interesting to note that the recently collected carbonaceous chondrite<sup>\*\*\*</sup> (Murchison) contained traces of pyridine.

---

\* K. Dressler, in "Interstellar Grains", J. M. Greenberg, Ed., NASA Publication, NASA SP-140 (1967).

\*\* E. M. Purcell, Ap. J., 158, 433 (1969).

\*\*\* News Notes, Sky and Telescope, 138, 388 (Dec. 1969).

## SECTION 4

### CONCLUSION AND SUMMARY

#### 4.1 CONCLUSION AND SUMMARY

An extensive experimental program was undertaken in an attempt to match the 25 optical diffuse interstellar lines. This program involved an experimental survey of hundreds of organic compounds and detailed studies of various techniques for suspending these molecules. We proceed in steps by successive analytic surveys and concomitant examinations of all the associated astronomical evidence which led to a narrow range of stable porphyrin compounds. This report is an attempt to show the total amount of experimental effort expended and the torturous path that had to be taken, leading to the final result of isolating a single molecular species (molecule  $\chi$ ) whose strongest absorption feature in the visible region (the Soret band) matched precisely the strongest diffuse interstellar line at 4428Å. In addition, 15 other lines were matched in the visible and six in the IR region of the spectrum. An energy level diagram was constructed where 19 transitions are consistent with vibronic transitions associated with molecule  $\chi$  and six transitions are characteristic of a closely related (yet undetermined) molecule,  $\chi'$ , presumably  $\chi'$  molecule complex.\*\* From a Boltzmann type plot involving "sum of states" some sort of fictitious temperature was obtained for the two molecular species, strongly suggesting two distinct radiative regions for the molecules: The molecule  $\chi$  closest to the source of radiation has most of its higher vibronic states "population inverted", the other species (TBP?) has an effective "radiative temperature" of 1000°K. It should be noted that the molecules  $\chi$  (and or TBP) are stable up to about 850°K (thermal) and that they do not get destroyed below these temperatures but sublime. This ability to survive adverse radiative

\*For H.D. 183143.

\*\*Dimer, Trimer of  $\chi$ .

environments must account for its dominance in certain regions of the galaxy where complex astroorganic synthesis is in progress.

Since molecule  $\chi$  is unusually large, much larger than anything heretofore identified in outer space, the question of uniqueness for the identification must be examined carefully. Such a calculation would involve the a priori probability of random accidental coincidences of (a) 16 + 6 spectral lines, (b) intensity and line width correlation, (c) assignment of 25 diffuse interstellar lines (with a precision of  $\pm 2 \text{ cm}^{-1}$ ) to two electronic states plus vibrational levels, (d) an extremely high degree of internal self-consistency of these energy level assignments using the strongest measured IR transitions of molecule  $\chi$ , (e) fundamental and multiples ( $n\nu$ ) of vibrational frequencies of  $\chi$ . This latter is the most striking, since  $n = 1, 3, 4, 5, 8$  for  $754 \text{ cm}^{-1}$ .

A calculation using very conservative probability estimates for each "coincidence" yields  $10^{50}:1$ . Certainly excellent odds compared to the total number of known organic and inorganic compounds, and comparable probability criteria that must be applied for definitive spectroscopic identification of any single organic compound.



## APPENDIX I

ABSTRACT OF PAPER PRESENTED AT  
AMERICAN ASTRONOMICAL SOCIETY, APRIL 1969  
A.J., No. 3, 246 (1969)

### Preliminary Low Temperature Absorption and Scattering Data of Organic Powders Simulating Interstellar Dust\*

Fred M. Johnson  
EOS Division of Xerox Corporation  
Pasadena, California 91107

Gordon W. Hodgson  
Stanford University  
Stanford, California 94305

Diffuse interstellar absorption lines may be due to organic substances in interstellar space. To test this possibility exploratory experiments were carried out to simulate interstellar absorption and scattering by measuring the wavelength dependence of the transmission of light through suspensions of stable aromatic compounds in various matrices. Measurements were made under conditions of fine dispersion in the solid state, at low temperature, and in the presence of mineral substances. Pyrene, perylene and other polycyclic aromatic hydrocarbons, and carbazole, porphyrins and other nitrogen containing aromatics, showed spectra in the visible range significantly different from the familiar corresponding spectra in solution. Generally, the short wavelength absorptions were suppressed and new bands appeared at longer wavelengths. For example, the Soret band of porphin at 385 nm became much less intense; in the case of perylene, a new band emerged at about 460 nm with an intensity comparable to that of the customary bands in the 400 to 430 nm range. Lowering of the temperature generally caused some of the lines to sharpen and to shift to the red by about 10 nm. Admixture of silicate and carbonate minerals generally weakened the absorption spectra of the

---

\* This work was supported by NASA under Contract No. NASW1803

organic compounds and increased the Mie scattering. Similar effects were observed for the admixture of dust from Orgueil and Murray carbonaceous chondrites as representatives of extra-terrestrial mineral matrices.

Scientific Report No. 1

BISPYRIDYLMAGNESIUMTETRABENZOPORPHINE ( $\chi$ )

AN INTERSTELLAR MOLECULE

(Submitted for publication to Science)

ABSTRACT

Chemical identification of interstellar molecule  $\chi$  is based on exact coincidence of measured low temperature absorption lines with astronomically observed diffuse interstellar lines. Molecule  $\chi$  has high thermodynamic stability. Its astrosynthesis and its possible subsequent role as precursor for porphyrin skeletons in the biosphere are outlined.

Astronomers estimate that 1.2 percent of interstellar matter is in the form of dust (1). Spectral studies of distant stars in the galactic plane reveal sharp interstellar absorption lines in the visible region which have been identified with the molecules CH and CN. Diffuse lines in such interstellar spectra (1) have eluded identification for some 40 years.

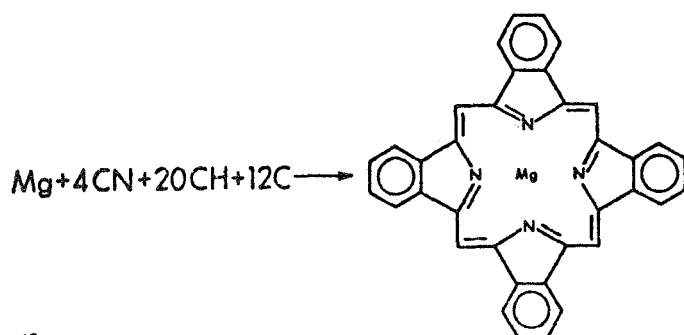
Employing low temperature techniques, we have scanned the spectra of a wide array of substances in an effort to correlate the known interstellar spectra and more recent astronomical observations (2) with a defined molecular structure.

The possibility that complex molecules (3) composed of carbon, hydrogen, and nitrogen might constitute these "grains" was first suggested in 1965. The search was narrowed to the porphyrin family (4, 5) in 1966. The history of this endeavor is extensive (6, 7).

We now wish to describe evidence for the assignment of the diffuse interstellar lines to the dipyrindine complex of magnesiumtetraabenzoporphine ("X", Fig. 1). We also comment briefly upon the thermodynamic and chemical properties of X that are consonant with its astrosynthesis and upon the prebiotic implications of its existence. Absorption and emission spectroscopic measurements of X at 77°K in inert matrices provide distinctive lines. Table 1 gives the major lines whose peak absorptions coincide, within the precision of our measurements, with the major interstellar lines. The ratio of line intensities (X<sub>4428</sub>/X<sub>6284</sub>) agrees with the intensities of the interstellar lines. The width of the 4428 Å line was shown to be concentration dependent. Hence the isolated molecule in vacuum could well have a narrower line width. On the other hand, the 6174 Å line was narrower in our experimental measurements than given by astronomical data. Six precision measurements of X in different matrices were performed on the Soret absorption line of which Fig. 2 is a typical microdensitometer trace from an exposed plate. Data was

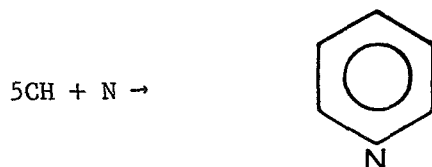
recorded on plates using a 3/4-m Jarrell-Ash spectrometer, (dispersion of 20 Å/mm) as well as by means of a specially constructed optical system comprising a chopped light source, sample in special dewar, scanning spectrophotometer and phase sensitive detection. Either a 300W bulb or a xenon arc lamp provided the continuum background radiation. No difference in the absorption peak (to within  $\pm 1$  Å) could be detected using either technique. Possible matrix shifts of the absorption lines must be less than 1-2 Å, since no shifts could be detected using a dozen variations. The intense  $\pi \rightarrow \pi^*$  Soret transition,  $f \sim 1$ , at 4428 Å accounts for its dominance in the interstellar spectrum. The chemical stability of the compound was explored by heating a quantity of X powder to over 500°C in vacuum in a molecular beam oven and collecting the effluent on a glass plate, 6 in. from the orifice. The green-colored deposit exhibited absorption spectra characteristic of X. Another experiment involved heating X molecules to 500-600°C in a quartz cell in order to study their absorption spectrum. A characteristic green vapor was obtained; i.e., the band at 6350 Å was measured, thus providing part of its signature. However, no sharp lines, not even the Soret band, are exhibited under these conditions, in agreement with theoretical considerations (8).

Our model for the astrosynthesis of X molecules is related to astronomical observations of IR circumstellar objects. Organic synthesis proceeds during the early stages of star formation (and based on the known values of atom abundances (1) relative to hydrogen, log 12; carbon, log 8.48; nitrogen, log 7.96; magnesium, log 7.46; iron, log 6.90) via a coalescence of atomic units through a cooling temperature gradient resulting in the most thermodynamically stable molecular grouping of the entities that are present (9). The overall stoichiometry for the astrosynthesis may be formulated as:



36447

A stepwise process can easily be envisioned in which the metal guides the synthesis by initially coordinating with four cyano moieties. The pyridine moieties may be synthesized on the metal or adjoin after the magnesium tetrabenzoporphine is intact. This highly stable heterocycle might easily be formed by a related condensation (for example)

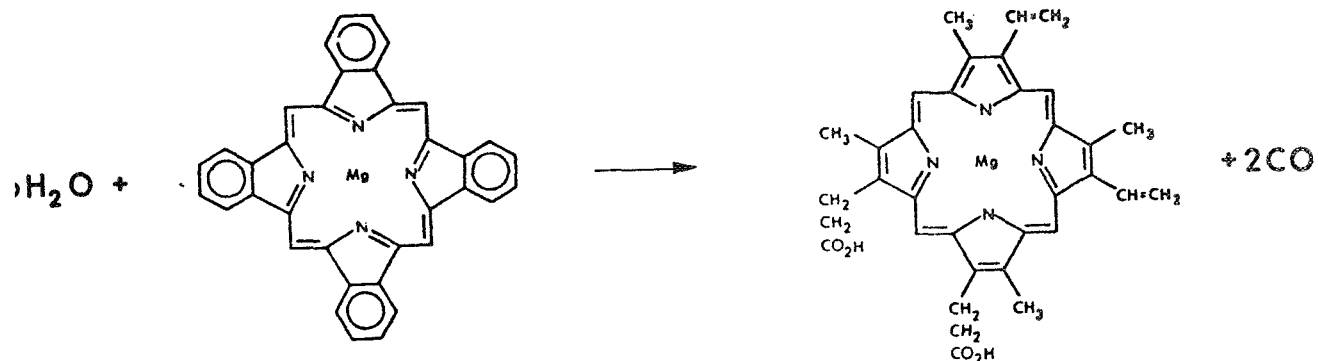


and our results predict that pyridine and benzene



should also be detected as interstellar molecules.

It is most significant that the tetrabenzoporphine nucleus contains the necessary number of carbon atoms to be a prebiotic chemical precursor for porphyrins skeletons currently present in the biosphere. For example, protoporphyrin complexes might well result from TBP compounds under drastic chemical conditions:



We are exploring the implications of these finds at all levels.

Fred M. Johnson, C. E. Castro  
 Department of Quantum Electronics,  
 Electro-Optical Systems, A Division  
 of Xerox Corporation, Pasadena,  
 California 91107, and the Department  
 of Nematology, University of  
 California, Riverside, California 92502

#### REFERENCES

1. C. W. Allen, "Astrophysical Quantities," (2nd Ed., Univ. of London Press, 1964) pp. 251-254, 30.
2. F. M. Johnson, in conference on "Interstellar Grains," J. M. Greenberg Ed. (August 1965), NASA Publication NASA SP-140 (1967) pp. 229-240.
3. F. M. Johnson, 123rd Meeting Am. Astron. Soc., December 1966, Astron. J. 72, No. 3, April 1967.
4. F. M. Johnson, Bull. Am. Phys. Soc., Series II, 11, 24 (1966).
5. G. H. Herbig, "The Diffuse Interstellar Lines III." IAU Symposium No. 31, p. 85, 1967.
6. F. M. Johnson, "Interstellar Matter," in Vol. 17 "Use of Space Systems for Planetary Geology and Geophysics, R. D. Enzmann Ed., (Am. Astronautical Soc. Publications Office, Tarzana, California, May 1967) pp. 51-65.
7. M. Bixon and J. Jortner, "Intramolecular Radiationless Transitions," J. Chem. Phys. 48, 715 (1968).



# LABORATORY MEASUREMENTS ON MOLECULE

AT 77°K

No. of Measurements	Laboratory Measurements		Astronomical Data*	
	$\lambda$	$\lambda$ Width $\lambda$	$\lambda$	Width $\lambda$
6	a	4428 $\pm$ 2 40	4428 <sup>**</sup>	20
3	a	6174 $\pm$ 2 10	6175	30
3	e	6284 $\pm$ 2 < 2	6284	4

\* Data kindly supplied by G. H. Herbig for H.D. 183143

(a) Absorption  
(e) Emission

\*\* G. H. Herbig, Zeits.f. Astrophysik, 64, 512 (1966).

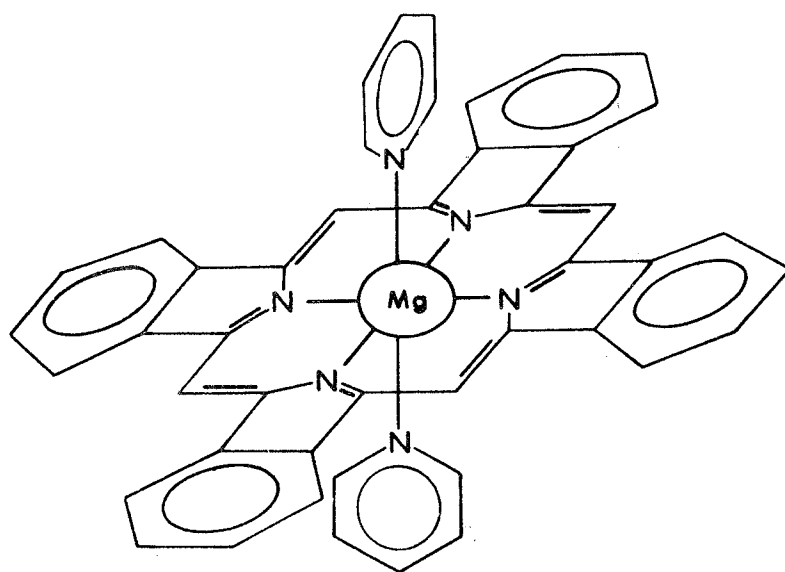


Figure 1. The Interstellar Molecule  $\chi$  ( $\text{MgC}_{46}\text{H}_{30}\text{N}_6$ )

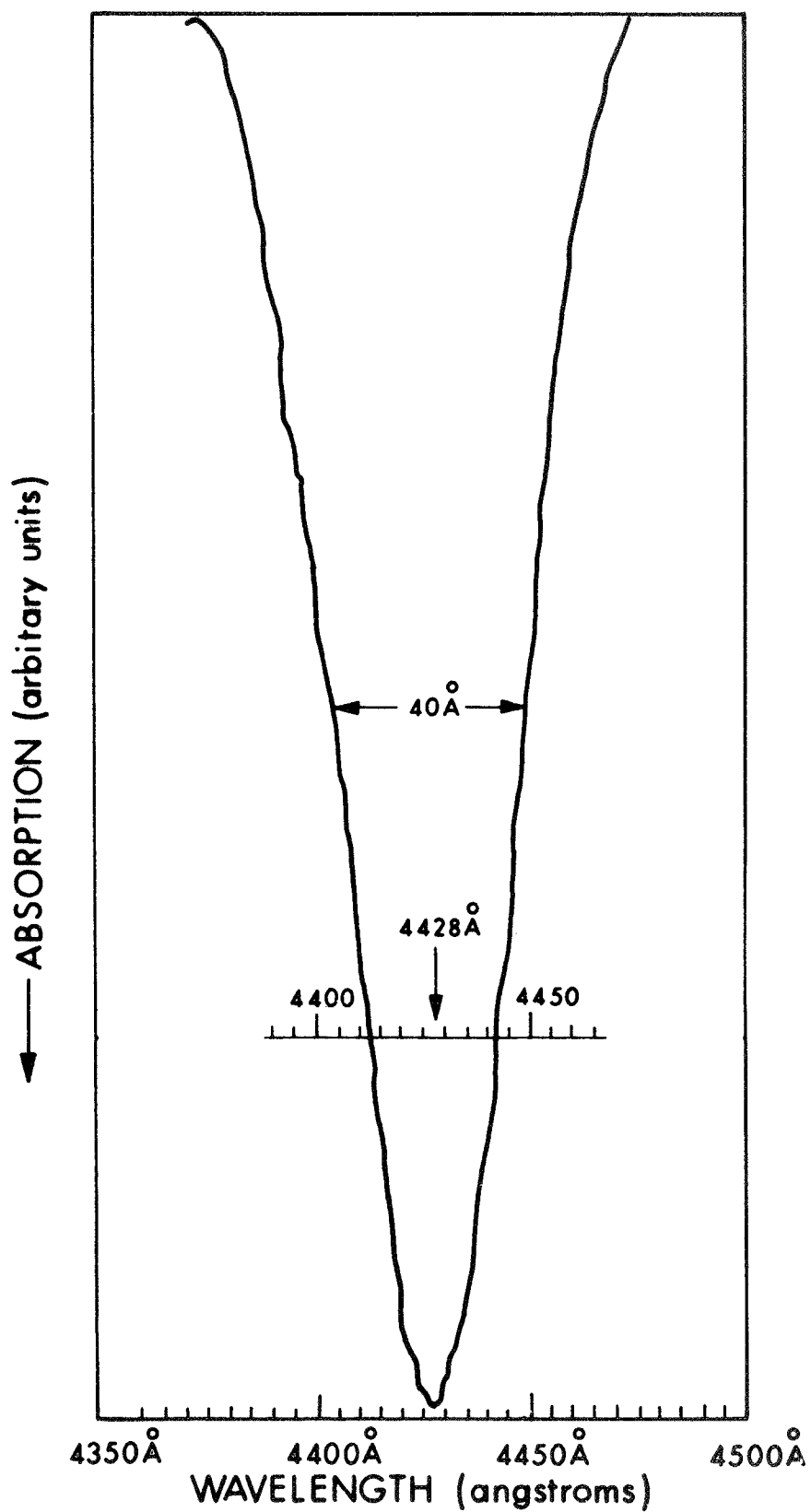


Figure 2. Laboratory Measurement Soret Band of Molecule X

NATIONAL AERONAUTICS AND SPACE ADMINISTRATION  
WASHINGTON, D. C. 20546  
OFFICIAL BUSINESS

FIRST CLASS MAIL



POSTAGE AND FEES PAID  
NATIONAL AERONAUTICS AND  
SPACE ADMINISTRATION

POSTMASTER: If Undeliverable (Section 158  
Postal Manual) Do Not Return

*"The aeronautical and space activities of the United States shall be conducted so as to contribute . . . to the expansion of human knowledge of phenomena in the atmosphere and space. The Administration shall provide for the widest practicable and appropriate dissemination of information concerning its activities and the results thereof."*

— NATIONAL AERONAUTICS AND SPACE ACT OF 1958

## NASA SCIENTIFIC AND TECHNICAL PUBLICATIONS

**TECHNICAL REPORTS:** Scientific and technical information considered important, complete, and a lasting contribution to existing knowledge.

**TECHNICAL NOTES:** Information less broad in scope but nevertheless of importance as a contribution to existing knowledge.

**TECHNICAL MEMORANDUMS:** Information receiving limited distribution because of preliminary data, security classification, or other reasons.

**CONTRACTOR REPORTS:** Scientific and technical information generated under a NASA contract or grant and considered an important contribution to existing knowledge.

**TECHNICAL TRANSLATIONS:** Information published in a foreign language considered to merit NASA distribution in English.

**SPECIAL PUBLICATIONS:** Information derived from or of value to NASA activities. Publications include conference proceedings, monographs, data compilations, handbooks, sourcebooks, and special bibliographies.

**TECHNOLOGY UTILIZATION PUBLICATIONS:** Information on technology used by NASA that may be of particular interest in commercial and other non-aerospace applications. Publications include Tech Briefs, Technology Utilization Reports and Technology Surveys.

*Details on the availability of these publications may be obtained from:*

SCIENTIFIC AND TECHNICAL INFORMATION DIVISION  
NATIONAL AERONAUTICS AND SPACE ADMINISTRATION  
Washington, D.C. 20546